Table 1. Aminoglycoside resistance pattern conferred by G1405 16S rRNA methylase.

Drug	Susceptibility
4,6-disubstituted DOS	Highly resistant
Gentamicin	Highly resistant
Tobramycin	Resistant, highly resistant
Amikacin	Highly resistant
4,5-disubstituted DOS; neomycin	Susceptible
Monosubstituted DOS; apramycin	Susceptible
No DOS ring; streptomycin	Susceptible

NOTE. DOS, deoxystreptamine.

the MICs of tobramycin for the clinical strains that produce 16S rRNA methylase usually range between 512 and 1024 μg/mL or greater. This pattern of resistance resembles that of the methylase of *M. purpurea*, which is known to methylate residue G1405, as discussed above. Recently, residue G1405 of 16S rRNA in the 30S ribosomal subunit was confirmed as the site of methylation by ArmA using primer extension method (figure 2) [19]. No methylase that modifies residue A1408 has been reported in gram-negative pathogens at this time.

PREVALENCE OF 16S rRNA METHYLASE–MEDIATED RESISTANCE

Data on the prevalence of aminoglycoside resistance mediated by 16S rRNA methylation among gram-negative bacilli is still scarce. The prevalence of RmtA among clinical isolates of *P. aeruginosa* in Japan was estimated to be at least 0.4% during a national surveillance when screened by high-level multiple-aminoglycoside resistance followed by PCR confirmation [5]. Subsequently, RmtB has been detected in various species belonging to the family *Enterobacteriaceae*, including *K. pneumoniae, Klebsiella oxytoca, E. coli,* and *C. freundii* in Japan, Taiwan, South Korea, China, and Belgium [20—25]. ArmA, which was initially found in *C. freundii* and later characterized in *K. pneumoniae,* has also been identified in clinical isolates of *E. coli, S. marcescens, Enterobacter cloacae, Salmonella enterica, Shigella flexneri,* and *Acinetobacter* species from various countries in East Asia and Eastern and Western Europe (table 2) [14, 20–23]. A recent report from a university hospital in Taiwan estimated the prevalence of ArmA and RmtB to be 0.9% and 0.3%, respectively, among *K. pneumoniae* and *E. coli* when screened by resistance to amikacin and confirmed by PCR [22]. RmtA and RmtD have only been reported from *P. aeruginosa* in Japan and Brazil, respectively [5, 18, 21]. These findings indicate that 16S rRNA methylase genes are already disseminated globally among pathogenic gram-negative bacilli, although the overall prevalence appears to remain low.

Strains producing 16S rRNA methylase have been reported from livestock, as well. Plasmid-mediated *armA* and *rmtB* genes have been identified from *E. coli* in swine from Spain and China, respectively [26, 25]. A large amount of aminoglycosides, including kanamycin, gentamicin, apramycin, and streptomycin, has been consumed in veterinary medicine. This may have served as a selective pressure for enteric gram-negative organisms to acquire 16S rRNA methylase genes, possibly from nonpathogenic environmental actinomycetes that intrinsically produced aminoglycosides or similar 16S rRNA inhibitors, and then maintain and spread them to humans through the food supply chains. Monitoring for high-level aminoglycoside resistance among gram-negative pathogens mediated by this new resistance mechanism would, therefore, be important in livestock breeding environments, as well.

Table 2. Genetic association and geographic distribution of 16S rRNA methylase genes.

16S rRNA methylase gene	Guanine cytosine content, %	Molecular weight of product, kDa	IS or transposon	Associated β-lactamase genes	Bacterial species (country or countries)	Country, reference(s)
rmtA	55.4	27.4	IS*6100*, *κγ* element, Tn*4051*		*Pseudomonas aeruginosa* (J)	J [5, 21]
rmtB	55.6	27.4	Tn*3*	bla_{TEM-1}, $bla_{CTX-M-14}$	*Serratia marcescens* (J), *Escherichia coli* (J, T, C, Be), *Klebsiella pneumoniae* (J, T, K), *Klebsiella oxytoca* (J), *Citrobacter freundii* (K)	J [15], T [22], K [20, 23], C (DQ345788), Be [24]
rmtC	41.1	32.1	IS*Ecp1*		*Proteus mirabilis* (J)	J [16]
rmtD	59.3	27.7	IS*CR*	bla_{SPM-1}	*P. aeruginosa* (Br)	Br [18]
armA	30.4	30.2	IS*26*, Tn*1548*	$bla_{CTX-M-3}$	*S. marcescens* (J, F, K), *C. freundii* (F, K, F, Bu), *Citrobacter amalonaticus* (Be), *K. pneumoniae* (F, S,T, K, Bu, Be), *K. oxytoca* (Bu), *E. coli* (J, T, S, F, Bu, Be), *Enterobacter cloacae* (F, K, Be), *Enterobacter aerogenes* (Bu, Be), *P. mirabilis* (F), *Salmonella enterica* Enteritidis (Bu), *S. enterica* Oranienburg (P), *Shigella flexneri* (Bu), *Acinetobacter* species (J, K)	P (AY522431) [14], Bu [14], F [14], S [26], Be [24], J [21], T [22], K [20, 23]

NOTE. DQ345788 and AY522431 are European Molecular Biology Laboratory and GenBank accession numbers. Be, Belgium; Br, Brazil; Bu, Bulgaria; C, China; F, France; I, India; IS, insertion sequence; J, Japan; K, South Korea; P, Poland; S, Spain; T, Taiwan.

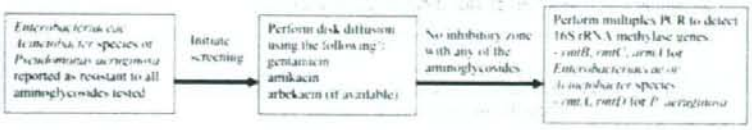

Figure 3. Suggested approach in identifying organisms producing 16S rRNA methylase. *Alternatively, MICs of 256 μg/mL to all aminoglycosides tested may be used.

CLINICAL IMPLICATION OF AMINOGLYCOSIDE RESISTANCE DUE TO 16S rRNA METHYLATION

Despite its currently low prevalence, the global spread of gram-negative bacilli producing 16S rRNA methylase is concerning for several reasons. First, these gram-negative bacilli show a very high level of resistance to most clinically useful aminoglycosides, including gentamicin, tobramycin, and amikacin, which cannot be overcome by dose adjustments. Second, all of the structural genes of known 16S rRNA methylases are associated with mobile genetic elements, such as transposon, some of which have been proven functional, providing them with the means to spread horizontally to other strains and species. Third, these organisms appear to possess a high potential for developing multidrug resistance, especially via acquisition of various β-lactamase genes. Of 35 ArmA- and RmtB-positive clinical isolates, 33 produced CTX-M- or SHV-type extended-spectrum β-lactamases (ESBLs) in a Taiwanese university hospital [22]. Similar observations have also been made in South Korea [20]. It has been reported that the structural gene for ArmA, the most prevalent methylase thus far, is located on a composite transposon Tn*1548* on a transferable plasmid and is frequently associated with CTX-M-3–type ESBL genes [14]. Production of CTX-M-9–type ESBLs is seen in many strains with RmtB [22] (K. Yamane, unpublished data). RmtD was initially reported in a *P. aeruginosa* strain that coproduced SPM-1 metallo-β-lactamase, which is endemic in Brazil. The latter combination would render ineffective a potent double-coverage regimen of carbapenem plus aminoglycoside. Currently, there are no data regarding clinical outcome in patients infected with these organisms. Nonetheless, it would be prudent to pay careful attention to the antibiogram and to maintain a low threshold to screen for ESBL production when these 16S rRNA methylase–producing gram-negative bacteria are encountered in clinical situations. Contact precautions should be used for patients when coproduction of 16S rRNA methylase and ESBL or metallo-β-lactamase is highly suspected or confirmed.

DETECTION OF AMINOGLYCOSIDE RESISTANCE DUE TO 16S rRNA METHYLATION

Screening for 16S rRNA methylase–producing organisms may be considered for epidemiologic purposes when nosocomial or foodborne spread of such bacteria is suspected. Detection of this resistance mechanism may pose a challenge in clinical laboratories. Gram-negative bacilli commonly produce aminoglycoside-modifying enzymes, such as acetyltransferases, nucleotidyltransferases, and phosphotransferases. When >1 of these enzymes are produced in single organisms, they could readily become resistant to multiple aminoglycosides. The hallmark of resistance mediated by 16S rRNA methylase that methylates residue G1405 is the very high level of resistance to all parenterally formulated aminoglycosides (MIC is typically ≥256 μg/mL), except streptomycin. This, however, may not be discernible in routine susceptibility testing conducted in the clinical laboratory, especially when automated susceptibility testing systems are used that only measure MICs close to the breakpoints of each aminoglycoside. One unique characteristic of these methylases is the high-level resistance to arbekacin that they confer. Arbekacin is a semisynthetic aminoglycoside derived from dibekacin [27]. It has activity against staphylococci,

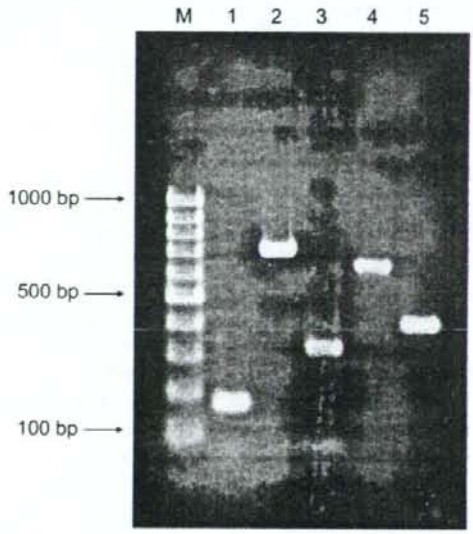

Figure 4. Electrophoresis profile of the PCR products. *Lane M*, 100–base pair (bp) marker; *lane 1, rmtB; lane 2, rmtC; lane 3, armA; lane 4, rmtA; lane 5, rmtD.*

Table 3. Primers for detection of 16S rRNA methylase genes.

Species, gene, primer	Sequence (5′→3′)	Amplicon size, base pairs
Enterobacteriaceae and *Acinetobacter* species		
rmtB		
rmtB-F	GCT TTC TGC GGG CGA TGT AA	173
rmtB-R	ATG CAA TGC CGC GCT CGT AT	
rmtC		
rmtC-F	CGA AGA AGT AAC AGC CAA AG	711
rmtC-R	ATC CCA ACA TCT CTC CCA CT	
armA		
armA-F	ATT CTG CCT ATC CTA ATT GG	315
armA-R	ACC TAT ACT TTA TCG TCG TC	
Pseudomonas aeruginosa		
rmtA		
rmtA-F	CTA GCG TCC ATC CTT TCC TC	635
rmtA-R	TTG CTT CCA TGC CCT TGC C	
rmtD		
rmtD-F	CGG CAC GCG ATT GGG AAG C	401
rmtD-R	CGG AAA CGA TGC GAC GAT	

NOTE. Both PCR for *rmtB*, *rmtC*, and *armA* and PCR for *rmtA* and *rmtD* may be performed in a mutiplex protocol. Thermal cycling condition is as follows: initial denaturation at 96°C for 5 min, followed by 30 cycles at 96°C for 30 s, at 55°C for 30 s, at 72°C for 1 min, with a final extension at 72°C for 5 min.

as well as against gram-negative bacteria, and it is currently approved only for treatment of multidrug-resistant *Staphylococcus aureus* infections in Japan. It is generally stable against the actions of aminoglycoside-modifying enzymes, with the exception of the bifunctional enzyme AAC(6′)/APH(2″), which is known to be produced by some multidrug-resistant *S. aureus* and enterococcal strains, and it may result in low-level arbekacin resistance. However, arbekacin is not readily available in many instances. Therefore, we propose the following approach in screening for 16S rRNA methylase production (figure 3). When a strain belonging to the family *Enterobacteriaceae* or glucose nonfermentative species, such as *P. aeruginosa* or *Acinetobacter* species, meets the criteria set forth by the Clinical and Laboratory Standards Institute for resistance to multiple aminoglycosides, disk diffusion test using gentamicin, amikacin, and arbekacin (if available) may be performed. Production of 16S rRNA methylase is suspected when no or little inhibitory zone is observed with any of the aminoglycoside disks. The addition of an arbekacin disk is desirable, because it raises the positive predictive value of this method to ≥90%, compared with ~60% when performed only with amikacin [20]. Alternatively, if the MICs of these aminoglycosides are to be used, a cutoff value of 256 μg/mL appears to provide excellent positive predictive value. All of the RmtA-, RmtB-, RmtC-, RmtD- and ArmA-producing isolates that we have tested to date have had MICs of these aminoglycosides ≥256 μg/mL—an observation confirmed elsewhere [20]. Currently, PCR is the only confirmatory method available. Multiplex PCR may be performed for *armA*, *rmtB*, and *rmtC* in strains belonging to the family *Enterobacteriaceae* and *Acinetobacter* species and for *rmtA* and *rmtD* in *P. aeruginosa* (figure 4). Recommended primers and thermal cycling conditions are listed in table 3. Of note, some other glucose nonfermentative organisms, such as *Stenotrophomonas maltophilia* and *Burkholderia cepacia*, may also present with panaminoglycoside-resistant phenotype, but the mechanism of this resistance has not been elucidated.

CONCLUSIONS

Methylation of the 16S rRNA in the 30S ribosomal subunit confers high-level resistance to most clinically useful aminoglycosides by inhibiting their access to the site of action. Gram-negative pathogens possessing this mechanism were first reported in 2003 and are increasingly reported worldwide. The organisms that produce 16S rRNA methylase are often multidrug resistant, especially against broad-spectrum β-lactams via production of ESBLs or metallo-β-lactamases, a process that is likely to be facilitated by the association of 16S rRNA methylase genes with genetic recombination systems. Although the clinical outcome for patients infected with these organisms is still unknown, early identification of the resistance mechanisms will be helpful in optimizing antimicrobial therapy and infection-control measures. A 2-tiered approach, consisting of disk diffusion tests followed by PCR confirmation, is recommended for detection of 16S rRNA methylase-mediated resistance.

Acknowledgments

We thank Dr. Kunikazu Yamane and Dr. Jun-ichi Wachino for their contribution to this article.

Financial support. Principal data on plasmid-mediated 16S rRNA methylases demonstrated in this article were obtained by a series of investigations supported by the Ministry of Health, Labor and Welfare, Japan.

Potential conflicts of interest. All authors: no conflicts.

References

1. Magnet S, Blanchard JS. Molecular insights into aminoglycoside action and resistance. Chem Rev **2005**; 105:477–98.
2. Shaw KJ, Rather PN, Hare RS, Miller GH. Molecular genetics of aminoglycoside resistance genes and familial relationships of the aminoglycoside-modifying enzymes. Microbiol Rev **1993**; 57:138–63.
3. Cundliffe E. How antibiotic-producing organisms avoid suicide. Annu Rev Microbiol **1989**; 43:207–33.
4. Galimand M, Courvalin P, Lambert T. Plasmid-mediated high-level resistance to aminoglycosides in *Enterobacteriaceae* due to 16S rRNA methylation. Antimicrob Agents Chemother **2003**; 47:2565–71.
5. Yokoyama K, Doi Y, Yamane K, et al. Acquisition of 16S rRNA methylase gene in *Pseudomonas aeruginosa*. Lancet **2003**; 362:1888–93.
6. Poehlsgaard J, Douthwaite S. The bacterial ribosome as a target for antibiotics. Nat Rev Microbiol **2005**; 3:870–81.
7. The RNA Modification Database. Available at: http://library.med.utah.edu/RNAmods/. Accessed 15 May 2007.
8. O'Connor M, Thomas CL, Zimmermann RA, Dahlberg AE. Decoding fidelity at the ribosomal A and P sites: influence of mutations in three different regions of the decoding domain in 16S rRNA. Nucleic Acids Res **1997**; 25:1185–93.
9. van Buul CP, Visser W, van Knippenberg PH. Increased translational fidelity caused by the antibiotic kasugamycin and ribosomal ambiguity in mutants harbouring the *ksgA* gene. FEBS Lett **1984**; 177:119–24.
10. Beauclerk AA, Cundliffe E. Sites of action of two ribosomal RNA methylases responsible for resistance to aminoglycosides. J Mol Biol **1987**; 193:661–71.
11. DNA Data Bank of Japan. ClustalW Web page. Available at: http://www.ddbj.nig.ac.jp/search/clustalw-e.html. Accessed 8 May 2007.
12. Kotra LP, Haddad J, Mobashery S. Aminoglycosides: perspectives on mechanisms of action and resistance and strategies to counter resistance. Antimicrob Agents Chemother **2000**; 44:3249–56.
13. Yamane K, Doi Y, Yokoyama K, et al. Genetic environments of the *rmtA* gene in *Pseudomonas aeruginosa* clinical isolates. Antimicrob Agents Chemother **2004**; 48:2069–74.
14. Galimand M, Sabtcheva S, Courvalin P, Lambert T. Worldwide disseminated *armA* aminoglycoside resistance methylase gene is borne by composite transposon Tn*1548*. Antimicrob Agents Chemother **2005**; 49:2949–53.
15. Doi Y, Yokoyama K, Yamane K, et al. Plasmid-mediated 16S rRNA methylase in *Serratia marcescens* conferring high-level resistance to aminoglycosides. Antimicrob Agents Chemother **2004**; 48:491–6.
16. Wachino J, Yamane K, Shibayama K, et al. Novel plasmid-mediated 16S rRNA methylase, RmtC, found in a *Proteus mirabilis* isolate demonstrating extraordinary high-level resistance against various aminoglycosides. Antimicrob Agents Chemother **2006**; 50:178–84.
17. Wachino J, Yamane K, Kimura K, et al. Mode of transposition and expression of 16S rRNA methyltransferase gene *rmtC* accompanied by IS*Ecp1*. Antimicrob Agents Chemother **2006**; 50:3212–5.
18. Doi Y, de Oliveira Garcia D, Adams J, Paterson DL. Co-production of novel 16S rRNA methylase RmtD and metallo-β-lactamase SPM-1 in a panresistant *Pseudomonas aeruginosa* isolate from Brazil. Antimicrob Agents Chemother **2006**; 51:852–6.
19. Liou GF, Yoshizawa S, Courvalin P, Galimand M. Aminoglycoside resistance by ArmA-mediated ribosomal 16S methylation in human bacterial pathogens. J Mol Biol **2006**; 359:358–64.
20. Lee H, Yong D, Yum JH, et al. Dissemination of 16S rRNA methylase-mediated highly amikacin-resistant isolates of *Klebsiella pneumoniae* and *Acinetobacter baumannii* in Korea. Diagn Microbiol Infect Dis **2006**; 56:305–12.
21. Yamane K, Wachino J, Doi Y, Kurokawa H, Arakawa Y. Global spread of multiple aminoglycoside resistance genes. Emerg Infect Dis **2005**; 11:951–3.
22. Yan JJ, Wu JJ, Ko WC, et al. Plasmid-mediated 16S rRNA methylases conferring high-level aminoglycoside resistance in *Escherichia coli* and *Klebsiella pneumoniae* isolates from two Taiwanese hospitals. J Antimicrob Chemother **2004**; 54:1007–12.
23. Park YJ, Lee S, Yu JK, Woo GJ, Lee K, Arakawa Y. Co-production of 16S rRNA methylases and extended-spectrum β-lactamases in AmpC-producing *Enterobacter cloacae, Citrobacter freundii* and *Serratia marcescens* in Korea. J Antimicrob Chemother **2006**; 58:907–8.
24. Bogaerts P, Galimand M, Bauraing C, et al. Emergence of ArmA and RmtB aminoglycoside resistance 16S rRNA methylases in Belgium. J Antimicrob Chemother **2007**; 59:459–64.
25. Chen L, Chen ZL, Liu JH, et al. Emergence of RmtB methylase-producing Escherichia coli and Enterobacter cloacae isolates from pigs in China. J Antimicrob Chemother **2007**; 59:880–5.
26. Gonzalez-Zorn B, Teshager T, Casas M, et al. *armA* and aminoglycoside resistance in *Escherichia coli*. Emerg Infect Dis **2005**; 11:954–6.
27. Kondo S, Hotta K. Semisynthetic aminoglycoside antibiotics: development and enzymatic modifications. J Infect Chemother **1999**; 5:1–9.

16S rRNA Methylase–producing, Gram-negative Pathogens, Japan

Kunikazu Yamane,* Jun-ichi Wachino,* Satowa Suzuki,* Naohiro Shibata,* Haru Kato,* Keigo Shibayama,* Kouji Kimura,* Kumiko Kai,* Satoshi Ishikawa,* Yoshiyuki Ozawa,* Toshifumi Konda,* and Yoshichika Arakawa*

To investigate the exact isolation frequency of 16S rRNA methylase–producing, gram-negative pathogenic bacteria, we tested 87,626 clinical isolates from 169 hospitals. Twenty-six strains from 16 hospitals harbored 16S rRNA methylase genes, which suggests sparse but diffuse spread of pan-aminoglycoside–resistant microbes in Japan.

Broad-spectrum β-lactams and fluoroquinolones have been widely prescribed in the treatment of gram-negative bacterial infections; as a result, resistance to these antimicrobial agents has developed in some species. Although these agents are not immune to an increasing number of resistance mechanisms, they remain relatively potent and continue to be essential antimicrobial drugs for treating life-threatening bacterial infections.

Although the production of aminoglycoside-modifying enzymes is the most common mechanism of resistance in aminoglycosides, the emergence of pan-aminoglycoside–resistant, 16S rRNA methylase–producing, gram-negative bacteria has been increasingly reported in recent years. Five types of plasmid-mediated 16S rRNA methylases (ArmA, RmtA, RmtB, RmtC, and RmtD) have so far been identified in east Asia, Europe, and South America (*1*–*7*). RmtA was first identified in 2001 in Japan (*3*) and has so far been identified exclusively in *Pseudomonas aeruginosa* (*8*). RmtC was subsequently identified only in *Proteus mirabilis* (*4*). RmtB has been found among various gram-negative bacterial species, including *Serratia marcescens*, *Escherichia coli*, *Citrobacter freundii*, *Klebsiella pneumoniae*, and *Klebsiella oxytoca*, isolated in Japan, South Korea, and Taiwan (*2*,*5*,*6*,*9*). Another new 16S rRNA methylase was initially identified in *C. freundii* in Poland, submitted to European Molecular Biology Laboratory (EMBL)/GenBank in 2002 (accession no. AF550415), and later characterized and assigned as ArmA in *K. pneumoniae*, *E. coli*, *Enterobacter cloacae*, *Salmonella enterica*, and *Shigella flexneri* in France, Bulgaria, and Spain (*10*,*11*). Moreover, ArmA was also identified in *E. coli*, *K. pneumoniae*, *E. cloacae*, *C. freundii* and *S. marcescens* in South Korea, Japan, and Taiwan (*5*,*8*,*9*). This enzyme has also been identified in a glucose nonfermentative *Acinetobacter* sp. in South Korea and Japan (*6*,*8*). Quite recently, RmtD was newly identified in the SPM-1–producing *P. aeruginosa* strain PA0905, which was isolated in Brazil (*7*). In Japan, arbekacin, a semisynthetic aminoglycoside, has been approved for treatment of methicillin-resistant *Staphylococcus aureus* infections, and this agent is also very efficacious for gram-negative bacteria. However, 16S rRNA methylase–producing microbes can adapt to this agent, and its prescription may well be a selective pressure on the kind of microbes in the clinical environment. Thus, this investigation was conducted to determine the exact isolation frequency of 16S rRNA methylase–producing, gram-negative pathogenic bacteria in Japanese medical facilities and assess the possibility of the future prevalence of these hazardous microbes.

The Study

From September 1 to October 31, 2004, 169 medical facilities with in-house microbiology laboratories participated in this investigation. Clinical specimens were collected from inpatients and outpatients with suspected infections. Bacterial isolates that belonged to the family *Enterobacteriaceae* or were nonfermentors of glucose, for example, *P. aeruginosa* and *Acinetobacter* spp., were included in this study. A total of 87,626 clinical isolates were analyzed. The results are shown in Table 1.

Twenty-nine strains (17 *P. aeruginosa*, 4 *A. baumannii*, 3 *E. coli*, 2 *P. mirabilis*, 1 *E. cloacae*, 1 *K. pneumoniae*, and 1 *Enterobacter aerogenes*) that grew on LB agar plates supplemented with 500 mg of arbekacin per liter were subjected to the typing of 16S rRNA methylase genes by a multiplex PCR. Primers used for the PCR amplification of bacterial 16S rRNA methylase genes were the following: RMTA-F 5′-CTA GCG TCC ATC CTT TCC TC-3′ and RMTA-R 5′-TTT GCT TCC ATG CCC TTG CC-3′, which amplify a 635-bp DNA fragment within *rmtA* gene (*3*); RMTB-F 5′-GCT TTC TGC GGG CGA TGT AA-3′ and RMTB-R 5′-ATG CAA TGC CGC GCT CGT AT-3′, which amplify a 173-bp DNA fragment within *rmtB* (*2*); RMTC-F 5′-CGA AGA AGT AAC AGC CAA AG-3′ and RMTC-R 5′-ATC CCA ACA TCT CTC CCA CT-3′, which amplify a 711-bp DNA fragment within *rmtC* (*4*); and ARMA-F 5′-ATT CTG CCT ATC CTA ATT GG-3′ and ARMA-R 5′-ACC TAT ACT TTA TCG TCG TC-3′, which amplify a 315-bp DNA fragment within *armA* (accession

*National Institute of Infectious Diseases, Tokyo, Japan

Table 1. Gram-negative strains investigated during September and October, 2004

Bacterial species	Strains, n			
	Isolated	Resistant to all aminoglycosides tested	Harboring 16S rRNA methylase gene, n	Rate of 16S rRNA methylase-producing strains, %
Pseudomonas aeruginosa	18,037	384	14	0.08
Escherichia coli	14,701	39	3	0.02
Klebsiella spp.	12,293	11	1	0.008
Enterobacter spp.	6,398	26	2	0.03
Acinetobacter spp.	3,116	33	4	0.13
Serratia marcescens	3,009	14	0	0
Citrobacter spp.	2,422	1	0	0
Proteus spp.	2,389	8	2	0.08
Alcaligenes spp.	443	0	0	0
Other	24,818	8	0	0
Total	87,626	527	26	0.03

nos. AY220558 and AB117519). PCR results and clinical data from these 29 strains are summarized in the Table 2. Genes for 16S rRNA methylases were absent in 3 arbekacin high-level-resistant strains of *P. aeruginosa* by PCR analyses that used 4 sets of 16S rRNA methylase-specific primers. In these strains, simultaneous production of multiple aminoglycoside-modifying enzymes was suggested as reported previously (*12*). Twenty-six strains harboring any of the four 16S rRNA methylase genes were identified in 16 hospitals, with no apparent geographic convergence in the locations of the hospitals (Figure 1). In hospital L, 3 different bacterial species (*E. coli*, *E. aerogenes*, and *K. pneumoniae*) harbored the *armA* gene, which suggests probable conjugal transfer of *armA*-carrying plasmids among different bacterial species.

Pulsed-field gel electrophoresis (PFGE) was performed on 9 strains of *P. aeruginosa* and 3 strains of *A. baumannii* isolated from 4 separate hospitals where 16S

Table 2. Bacterial species and type of 16S rRNA methylase gene detected*

Strain no.	Bacterial species	PCR type of 16S rRNA methylase gene	Hospital	Clinical specimen
40	*Proteus mirabilis*	*rmtC*	A	Sputum
64	*Pseudomonas aeruginosa*	*rmtA*	B	Sputum
101	*P. aeruginosa*	*rmtA*	C	Otorrhea
103	*P. aeruginosa*	*rmtA*	C	Otorrhea
109	*P. aeruginosa*	*rmtA*	C	Otorrhea
113	*P. aeruginosa*	*rmtA*	D	Bile
127	*P. aeruginosa*	*rmtA*	D	Pharynx
157	*P. aeruginosa*	*rmtA*	D	Pharynx
158	*P. aeruginosa*	*rmtA*	D	Stool
231	*Acinetobacter baumannii*	*armA*	E	Wound
249	*P. aeruginosa*	*rmtA*	F	Pus
252	*P. aeruginosa*	*rmtA*	F	Pleural fluid
328	*P. mirabilis*	*rmtC*	G	Sputum
353	*P. aeruginosa*	*rmtA*	H	Sputum
386	*Escherichia coli*	*rmtB*	I	Urine
422	*P. aeruginosa*	UD	J	Urine
463	*P. aeruginosa*	*rmtA*	K	Urine
469	*E. coli*	*armA*	L	Skin
470	*Enterobacter aerogenes*	*armA*	L	Stool
471	*Klebsiella pneumoniae*	*armA*	L	Stool
479	*P. aeruginosa*	*rmtA*	M	Unknown
499	*E. coli*	*armA*	N	Urine
509	*Enterobacter cloacae*	*armA*	O	Urine
525	*P. aeruginosa*	UD	P	Urine
527	*P. aeruginosa*	UD	Q	Blood
593	*P. aeruginosa*	*rmtA*	R	Vaginal secretion
615	*A. baumannii*	*armA*	S	Sputum
617	*A. baumannii*	*armA*	S	Sputum
619	*A. baumannii*	*armA*	S	Pus

*Strains for which MIC of arbekacin was ≥512 mg/L are listed; UD, undetected.

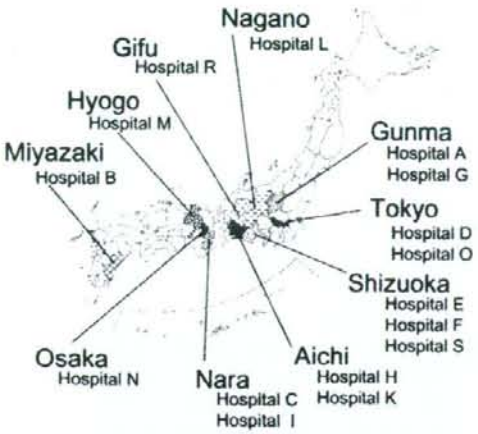

Figure 1. Geographic distribution of hospitals where 16S rRNA methylase gene-positive strains were isolated. Of 16 hospitals, 4 were located in the Kanto area (Gunma and Tokyo), 6 in the Chubu area (Aichi, Gifu, and Shizuoka), 1 in the Koushin-etsu area (Nagano), 4 in the Kinki area (Osaka, Nara, and Hyogo), and 1 in the Kyushu area (Miyazaki). This distribution suggests a sparse but diffuse spread of 16S rRNA methylase-producing, gram-negative pathogenic microbes in Japan. Bacterial species and type of 16S rRNA methylase identified in each hospital are shown in Table 2.

rRNA methylase genes were isolated (Figure 2). Genomic DNA preparations from *P. aeruginosa* and *A. baumannii* were digested with *Spe*I and *Sma*I, respectively. Clonality was inferred based on the criteria of Tenover et al. (*13*) Two of 3 *rmtA*-positive *P. aeruginosa* strains isolated in hospital C were estimated to be the same clone. Among 4 *rmtA*-positive *P. aeruginosa* isolates recovered in hospital D, 2 different clonal lineages were observed. This finding suggests possible conjugal transfers of *rmtA*-carrying plasmids among genetically different strains of *P. aeruginosa*. Three *armA* gene–harboring *A. baumannii* identified in hospital S were obviously the same clone. These findings imply probable nosocomial transmission of 16S rRNA methylase gene–harboring strains in hospitals C, D, and S, as well as frequent conjugal transfers of plasmids carrying 16S rRNA methylase genes among gram-negative pathogenic bacterial species.

MIC determinations were performed according to the guideline of the CLSI (formerly National Committee on Clinical Laboratory Standards). All 16S rRNA methylase-positive strains were highly resistant (MICs >1,024 mg/L) of all 4,6-disubstituted deoxystreptamine group aminoglycosides (Table 3). In contrast, resistance to streptomycin and neomycin varied. Three16S rRNA methylase gene-negative *P. aeruginosa* strains were also highly resistant to arbekacin, but the MICs of some of the 4,6-disubstituted deoxystreptamine group aminoglycosides were relatively lower (256–512 mg/L) for these strains than those for 16S rRNA methylase gene–positive strains (>1,024 mg/L). Strains harboring 16S rRNA methylase genes tended to show resistance to oxyimino-cephalosporins such as cefotaxime and ceftazidime as well, but were susceptible to imipenem. As reported for the *armA*- or *rmtB*-bearing strains, the presence of β-lactamase genes was suggested in cefotaxime-resistant strains, and indeed the $bla_{\text{CTX-M-14}}$ gene was detected in several *rmtB*-positive strains tested in our study (data not shown). Some of these strains also demonstrated resistance to fluoroquinolones (Table 3).

Conclusions

The overall isolation frequency of 16S rRNA methylase-gene-positive gram-negative bacilli was very low (0.03%) in Japanese medical facilities in 2004, with the highest rates seen in *P. aeruginosa* and *Acinetobacter* spp. at 0.08% and 0.13%, respectively. Twenty-six bacterial isolates carrying 1 of the four 16S rRNA methylase genes were recovered from 16 (9.5%) of 169 hospitals that participated in this nationwide investigation. Of the 169 hospitals, 162 hospitals had ≥200 beds, accounting for 5.9% of all Japanese hospitals of similar scale. This implies that 16S rRNA methylase–producing strains might have been present in >250 Japanese hospitals during the investigation period, which in turn suggests sparse but diffuse spread of 16S rRNA methylase producers in Japan. Since several

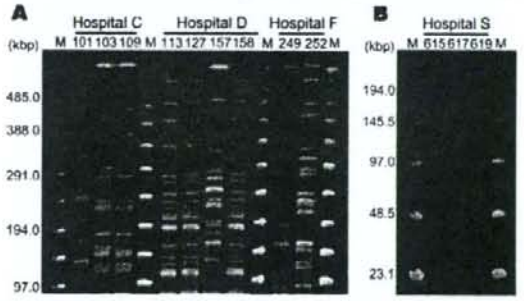

Figure 2. A) Pulsed-field gel electrophoresis (PFGE) fingerprinting patterns of *Spe*I-digested total DNA preparations from *Pseudomonas aeruginosa*. M, Lambda ladder PFGE molecular mass marker (Bio-Rad, Hercules, CA, USA). Strains 103 and 109 show similar patterns, which suggests probable nosocomial transmission of *rmtA*-positive strains in hospital C. Strains 113, 127, and 158 also demonstrate similar patterns, which implies possible nosocomial transmission in hospital D. However, 2 different PFGE patterns are observed in hospitals C, D, and F, which suggests transfer of plasmids carrying 16S rRNA-methylase genes among *P. aeruginosa* strains with different genetic backgrounds. B) *Sma*I-digested total DNA preparations from *Acinetobacter baumannii* isolated from hospital S. Three strains demonstrate the same PFGE pattern, which suggests probable nosocomial transmission of *armA*-positive *A. baumannii* in hospital S. M, lambda ladder low-range PFGE molecular mass marker (New England Biolabs, Ipswich, MA, USA).

Table 3. MICs of antimicrobial agents for arbekacin-resistant strains*†‡

Strain no.	MIC (mg/L)										
	ABK	AMK	TOB	ISP	GEN	SM	NEO	CTX	CAZ	IPM	CIP
40	>1,024	>1,024	>1,024	>1,024	>1,024	8	>1,024	<0.06	0.125	0.125	64
64	>1,024	>1,024	>1,024	>1,024	>1,024	8	>1,024	<0.06	0.5	0.125	64
101	>1,024	>1,024	>1,024	>1,024	>1,024	32	>1,024	8	2	0.5	32
103	>1,024	>1,024	>1,024	>1,024	>1,024	32	16	64	2	0.5	<0.06
109	>1,024	>1,024	>1,024	>1,024	>1,024	8	16	64	16	0.5	<0.06
113	>1,024	>1,024	>1,024	>1,024	>1,024	128	512	16	2	16	0.125
127	>1,024	>1,024	>1,024	>1,024	>1,024	128	128	16	2	16	<0.06
157	>1,024	>1,024	>1,024	>1,024	>1,024	32	32	64	4	2	0.5
158	>1,024	>1,024	>1,024	>1,024	>1,024	128	512	32	8	16	0.125
231	>1,024	>1,024	>1,024	>1,024	>1,024	>1,024	32	>128	128	4	16
249	>1,024	>1,024	>1,024	>1,024	>1,024	256	512	16	1	4	<0.06
252	>1,024	>1,024	>1,024	>1,024	>1,024	512	512	128	4	4	8
328	>1,024	>1,024	>1,024	>1,024	>1,024	8	512	>128	>128	2	32
353	>1,024	>1,024	>1,024	>1,024	>1,024	32	256	64	>128	4	32
386	>1,024	>1,024	>1,024	>1,024	>1,024	256	256	128	>128	0.5	>128
422	>1,024	>1,024	>1,024	256	>1,024	512	>1,024	>128	>128	8	128
463	>1,024	>1,024	>1,024	>1,024	>1,024	64	128	16	4	8	32
469	>1,024	>1,024	>1,024	>1,024	>1,024	64	32	>128	8	0.25	<0.06
470	>1,024	>1,024	>1,024	>1,024	>1,024	128	8	>128	>128	4	1
471	>1,024	>1,024	>1,024	>1,024	>1,024	64	8	128	4	0.25	<0.06
479	>1,024	>1,024	>1,024	>1,024	>1,024	256	1,024	64	4	0.25	0.25
499	>1,024	>1,024	>1,024	>1,024	>1,024	64	4	0.06	0.125	0.25	0.25
509	>1,024	>1,024	>1,024	>1,024	>1,024	64	1	>128	64	0.25	125
525	512	512	1,024	512	256	>1,024	>1,024	128	32	16	>128
527	1,024	512	1,024	>1,024	64	>1,024	>1,024	>128	>128	128	0.125
593	>1,024	>1,024	>1,024	>1,024	>1,024	128	64	>128	128	2	0.5
615	>1,024	>1,024	>1,024	>1,024	>1,024	>1,024	16	>128	>128	1	32
617	>1,024	>1,024	>1,024	>1,024	>1,024	>1,024	32	>128	>128	1	32
619	>1,024	>1,024	>1,024	>1,024	>1,024	>1,024	32	>128	>128	1	32

*ABK, arbekacin; AMK, amikacin; TOB, tobramycin; ISP, isepamicin; GEN, gentamicin; SM, streptomycin; NEO, neomycin; CTX, cefotaxime; CAZ, ceftazidime; IPM, imipenem; CIP, ciprofloxacin.
†MICs of kanamycin and sisomicin are not listed because values are >1,024 for all strain numbers.
‡See Table 2 for bacterial species and PCR type of 16S rRNA methylase gene of each strain number.

armA- or *rmtB*-positive strains have also been isolated in European and Asian countries, and given the potential for further dissemination, nationwide identification and ongoing surveillance of these isolates should be considered by all countries.

According to PFGE typing, nosocomial transmission of 16S rRNA methylase–producing *P. aeruginosa* and *A. baumannii* was suspected in 3 hospitals (hospitals C, D, and S). The banding patterns of *rmtA*-harboring *P. aeruginosa* isolated in hospitals C, D, and F were diverse, which excluded the possibility of an epidemic *P. aeruginosa* strain harboring the *rmtA* gene. Despite the observation of 2 different PFGE profiles among the 4 *P. aeruginosa* strains isolated in hospital D, they might share the same plasmids carrying the *rmtA* gene. For further characterization of genetic relations among *rmtA*-harboring *P. aeruginosa* strains, comparative analyses of plasmids and mobile elements that carry the *rmtA* gene (*14*) should also be pursued.

Nosocomial infections caused by multidrug-resistant, gram-negative bacteria have become a serious problem in clinical facilities. *P. aeruginosa* and *Acinetobacter* spp. have been especially efficient at developing multidrug resistance against broad-spectrum β-lactams, fluoroquinolones, and aminoglycosides (*3,6,7,9*). The identification of *armA* and *rmtB* genes in Europe and East Asia in both human (*1–11*) and livestock (*15;* EMBL/GenBank accession no. DQ345788) populations suggests that we must pay consistent attention to prevent further global proliferation. If 16S rRNA methylase–positive bacterial isolates disseminate widely and extensively, the high level of pan-aminoglycoside resistance will undoubtedly have an impact on illness, deaths, and costs of care in both clinical and livestock-breeding environments.

Acknowledgments

We thank all of the cooperating medical institutions for submitting the various bacterial strains to the National Reference Laboratory to allow this study.

Bacterial strains were collected and characterized with support from a grant (H16-Tokubetsu-027) from the Ministry of Health, Labor and Welfare, Japan. Precise molecular typing was

supported in part by a Grant-in-Aid (no. 16790318) for Young Scientists (B) from the Ministry of Education, Culture, Sports, Science and Technology, Japan.

Dr Yamane is a research scientist at the National Institute of Infectious Diseases, Japan. His research interests include infection control and the molecular mechanisms of antimicrobial resistance in nosocomial bacteria.

References

1. Galimand M, Courvalin P, Lambert T. Plasmid-mediated high-level resistance to aminoglycosides in *Enterobacteriaceae* due to 16S rRNA methylation. Antimicrob Agents Chemother. 2003;47:2565–71.
2. Doi Y, Yokoyama K, Yamane K, Wachino J, Shibata N, Yagi T, et al. Plasmid-mediated 16S rRNA methylase in *Serratia marcescens* conferring high-level resistance to aminoglycosides. Antimicrob Agents Chemother. 2004;48:491–6.
3. Yokoyama K, Doi Y, Yamane K, Kurokawa H, Shibata N, Shibayama K, et al. Acquisition of 16S rRNA methylase gene in *Pseudomonas aeruginosa*. Lancet. 2003;362:1888–93.
4. Wachino J, Yamane K, Shibayama K, Kurokawa H, Shibata N, Suzuki S, et al. Novel plasmid-mediated 16S rRNA methylase, RmtC, found in a *Proteus mirabilis* isolate demonstrating extraordinary high-level resistance against various aminoglycosides. Antimicrob Agents Chemother. 2006;50:178–84.
5. Park YJ, Lee S, Yu JK, Woo GJ, Lee K, Arakawa Y. Co-production of 16S rRNA methylases and extended-spectrum β-lactamases in AmpC-producing *Enterobacter cloacae*, *Citrobacter freundii* and *Serratia marcescens* in Korea. J Antimicrob Chemother. 2006;58:907–8.
6. Lee H, Yong D, Yum JH, Roh KH, Lee K, Yamane K, et al. Dissemination of 16S rRNA methylase-mediated highly amikacin-resistant isolates of *Klebsiella pneumoniae* and *Acinetobacter baumannii* in Korea. Diagn Microbiol Infect Dis. 2006;56:305–12.
7. Doi Y, de Oliveira Garcia D, Adams J, Paterson DL. Co-production of novel 16S rRNA methylase RmtD and metallo- β-lactamase SPM-1 in a panresistant *Pseudomonas aeruginosa* isolate from Brazil. Antimicrob Agents Chemother. 2007;51:8552–6.
8. Yamane K, Wachino J, Doi Y, Kurokawa H, Arakawa Y. Global spread of multiple-aminoglycoside-resistance genes. Emerg Infect Dis. 2005;11:951–3.
9. Yan JJ, Wu JJ, Ko WC, Tsai SH, Chuang CL, Wu HM, et al. Plasmid-mediated 16S rRNA methylases conferring high-level aminoglycoside resistance in *Escherichia coli* and *Klebsiella pneumoniae* isolates from two Taiwanese hospitals. J Antimicrob Chemother. 2004;54:1007–12.
10. Galimand M, Sabtcheva S, Courvalin P, Lambert T. Worldwide disseminated *arm.1* aminoglycoside resistance methylase gene is borne by composite transposon Tn*1548*. Antimicrob Agents Chemother. 2005;49:2949–53.
11. Gonzalez-Zorn B, Catalan A, Escudero JA, Dominguez L, Teshager T, Porrero C, et al. Genetic basis for dissemination of *armA*. J Antimicrob Chemother. 2005;56:583–5.
12. Doi Y, Wachino J, Yamane K, Shibata N, Yagi T, Shibayama K, et al. Spread of novel aminoglycoside resistance gene *aac(6')-Iad* among *Acinetobacter* clinical isolates in Japan. Antimicrob Agents Chemother. 2004;48:2075–80.
13. Tenover FC, Arbeit RD, Goering RV, Mickelsen PA, Murray BE, Persing DH, et al. Interpreting chromosomal DNA restriction patterns produced by pulsed-field gel electrophoresis: criteria for bacterial strain typing. J Clin Microbiol. 1995;33:2233–9.
14. Yamane K, Doi Y, Yokoyama K, Yagi T, Kurokawa H, Shibata N, et al. Genetic environments of the *rmtA* gene in *Pseudomonas aeruginosa* clinical isolates. Antimicrob Agents Chemother. 2004;48:2069–74.
15. Gonzalez-Zorn B, Teshager T, Casas M, Porrero MC, Moreno MA, Courvalin P, et al. *armA* and aminoglycoside resistance in *Escherichia coli*. Emerg Infect Dis. 2005;11:954–6.

Address for correspondence: Yoshichika Arakawa, Department of Bacterial Pathogenesis and Infection Control, National Institute of Infectious Diseases, 4-7-1 Gakuen, Musashi-Murayama, Tokyo 208-0011, Japan; email: yarakawa@nih.go.jp

ELSEVIER

INSTITUT PASTEUR

Microbes and Infection 9 (2007) 70–77

www.elsevier.com/locate/micinf

Original article

Contribution of GM-CSF on the enhancement of the T cell-stimulating activity of macrophages

Masahiko Makino*, Yumi Maeda, Yasuo Fukutomi, Tetsu Mukai

Department of Microbiology, Leprosy Research Center, National Institute of Infectious Diseases, 4-2-1 Aobacho, Higashimurayama, Tokyo 189-0002, Japan

Received 9 November 2005; accepted 10 October 2006
Available online 11 December 2006

Abstract

Mycobacterium leprae is an intracellular parasitic organism that multiplies in macrophages (MØ). It inhibits the fusion of mycobacterial phagosome with lysosome and induces interleukin (IL)-10 production from macrophages. However, macrophages are heterogenous in various aspects. We examined macrophages that differentiated from monocytes using either recombinant (r) granulocyte-MØ colony-stimulating factor (GM-CSF) (these MØ are named as GM-MØ) or rMØ colony-stimulating factor (M-CSF) (cells named as M-MØ) in terms of the T cell-stimulating activity. Although both macrophages phagocytosed the mycobacteria equally, GM-MØ infected with *M. leprae* and subsequently treated with IFN-γ- and CD40 ligand (L) stimulated T cells to produce interferon-gamma (IFN-γ), but M-MØ lacked the ability to stimulate T cells. While M-MØ mounted a massive IL-10 production, GM-MØ did not produce the cytokine on infection with *M. leprae*. *M. leprae*-infected, IFN-γ- and CD40L-treated GM-MØ expressed a higher level of HLA-DR and CD86 Ags than those of M-MØ, and expressed one of the dominant antigenic molecules of *M. leprae*, Major Membrane Protein-II on their surface. These results indicate that GM-CSF, but not M-CSF, contributes to the up-regulation of the T cell-stimulating activity of *M. leprae*-infected macrophages.

Keywords: Macrophage; *M. leprae*; GM-CSF; IFN-γ

1. Introduction

Mycobacterium leprae (*M. leprae*), a causative agent of human leprosy, is a representative parasitic pathogen that induces skin lesions and chronic progressive peripheral nerve injury, leading to systemic deformity [1,2]. Leprosy represents a clinical spectrum, in which clinical manifestations are associated with different levels of immune responses to *M. leprae* infection [3]. One representative type is a tuberculoid leprosy, in which patients exhibit innate and adaptive immunities to *M. leprae* and manifest a localized form of the disease with granuloma formation in infected tissues [4–6]. For the activation of an adaptive immunity, dendritic cells (DC) derived from inflammatory monocytes, play a central role [7,8]; and, in *in vitro* experiments, both $CD4^+$ and $CD8^+$ T cells are activated by DC infected with *M. leprae*, and these DC expressed Major Membrane Protein-II (MMP-II) as a dominant antigenic molecule [9,10]. Another representative manifestation is lepromatous leprosy, in which patients show reduced levels of host defense associated immunities and manifest a disseminated form of the disease with a broad spread of foamy MØ, in which an abundance of bacilli are usually involved [11,12]. *M. leprae* resides in the phagosome in MØ and replicates there without being digested by lysosomal enzymes [13]. Furthermore, *M. leprae* stimulates MØ to produce IL-10 [5,6] and suppresses the DC-mediated Ag-specific

Abbreviations: Ag, antigen; APC, Ag-presenting cells; BCG, *Mycobacterium bovis* BCG; DC, dendritic cells; GFP-BCG, BCG expressing GFP; GM-CSF, granulocyte-macrophage colony-stimulating factor; IFN-γ, interferon-gamma; IL, interleukin; L, ligand; mAb, monoclonal antibody; MØ, macrophages; M-CSF, MØ colony-stimulating factor; *M. leprae*, *Mycobacterium leprae*; MMP-II, Major Membrane Protein-II; PBMC, peripheral blood mononuclear cells; r, recombinant.

* Corresponding author. Tel.: +81 42 391 8059; fax: +81 42 391 8212.
E-mail address: mmaki@nih.go.jp (M. Makino).

1286-4579/$ - see front matter © 2006 Elsevier Masson SAS. All rights reserved.
doi:10.1016/j.micinf.2006.10.011

adaptive immunity [14,15]. These observations may indicate that the induction of intracellular processing of *M. leprae* and that of expression of molecules, such as MMP-II could lead to the activation of IFN-γ producing type 1 $CD4^+$ T cells. Another important element that should be considered for the full activation of T cells is the suppression of IL-10 production from *M. leprae*-infected MØ.

So far, a variety of methods and tools, including cytokines, have been used for the differentiation of MØ from human peripheral monocytes *in vitro* [16–18]. One representative MØ can be differentiated by using M-CSF, termed M-MØ, and another by using GM-CSF, termed GM-MØ. Both MØ represent different functions on infection with mycobacteria. However, much remains not fully understood with regard to *M. leprae* infection and the T cell-stimulating activity of these MØ.

In this report, we analyzed the characteristics of *M. leprae*-infected GM-MØ and M-MØ, and tried to develop immunological methods to enhance the MØ-mediated host defense activities against the bacteria.

2. Materials and methods

2.1. Preparation of cells and bacteria

Peripheral blood was obtained from healthy PPD-positive individuals under informed consent. We are aware that PPD-negative individuals would help to provide more information for our study; however, in Japan, most healthy individuals are PPD-positive, because *Mycobacterium bovis* BCG vaccination is compulsory for children (0–4 years old). Moreover, PPD-negative individuals in the Japanese population are those who do not respond to BCG vaccination, and therefore, it is likely that they suffer from some immune insufficiency. Therefore, these individuals cannot be used as controls for our experiments. Peripheral blood mononuclear cells (PBMC) were isolated using Ficoll-Paque Plus (Pharmacia, Uppsala, Sweden) and cryopreserved in liquid nitrogen until use, as previously described [19]. For preparation of peripheral monocytes, $CD3^+$ T cells were removed from either freshly isolated heparinized blood, or cryopreserved PBMC using immunomagnetic beads coated with anti-CD3 monoclonal antibody (mAb) (Dynabeads 450, Dynal, Oslo, Norway). The $CD3^-$ PBMC fraction was plated on collagen-coated plates and the non-plastic adherent cells were removed by extensive washing. The remaining adherent cells were used as monocytes [19]. MØ were differentiated by culturing monocytes in the presence of 20% fetal calf serum and either rM-CSF (R and D Systems, Abingdon, UK) (M-MØ) or rGM-CSF (Pepro Tech EC LTD, London, UK) (GM-MØ) [20]. Both GM-MØ and M-MØ were pulsed with *M. leprae*, treated with an optimal dose of IFN-γ on day 3 of culture, further treated with CD40L on day 4, and were used as a stimulator of T cells on day 5 [21]. *M. leprae* (Thai-53) was isolated from the footpads of BALB/c-*nu/nu* mice [22]. The isolated bacteria were counted by Shepard's method [22]. Killed *M. leprae* was prepared by heating the bacteria at 60 °C for 18 h. BCG (Pasteur strain) was cultured *in vitro* using Middlebrook 7H9 broth supplemented with 0.05% Tween 80 and albumin-dextrose-catalase. BCG expressing GFP was constructed as follows. The GFP sequence was amplified from pEGFP-1 vector (CLONTECH, Palo Alto, CA), and cloned into pMV261 [23]. Transformants were selected on a 7H10 plate containing 25 μg/ml kanamycin. The phagocytosis of BCG by GM-MØ and M-MØ after culture was determined using FACScalibur (Becton Dickinson Immunocytometry System, San Jose, CA). The multiplicity of infection (MOI) was determined based on the assumption that MØ were equally susceptible to infection with *M. leprae* [24].

2.2. Analysis of cell surface antigen (Ag)

The expression of cell surface Ag on MØ was analyzed using FACScalibur. Dead cells were eliminated from the analysis by staining with propidium iodide (Sigma Chemical Co., St. Louis, MO) and 1×10^4 live cells were analyzed. For analysis of cell surface Ag, the following mAbs were used: FITC-conjugated mAb against HLA-ABC (G46-2.6, PharMingen, San Diego, CA), HLA-DR (L243, PharMingen), CD14 (M5E2, BD Biosciences, San Jose, CA), TLR2 (TL2.3, Serotec, Oxford, UK), TLR4 (HTA125, Santa Cruz Biotech, Santa Cruz, CA), CD209 (DCN46, PharMingen), CD86 (FUN-1, PharMingen), and CD40 (5C3, PharMingen).

The expression of MMP-II, which is one of the dominant antigenic molecules of *M. leprae* [9] on *M. leprae*-infected MØ was determined using the mAb (IgM, kappa) against MMP-II, followed by FITC-conjugated anti-mouse Igs Ab (Tago-immunologicals, Camarillo, CA).

2.3. APC function of M. leprae-infected MØ

The ability of *M. leprae*-infected MØ to stimulate T cells was assessed using an autologous MØ-T cell co-culture as previously described [24,25]. Freshly thawed PBMC were depleted of $CD56^+$, MHC class II^+ and $CD8^+$ cells by using magnetic beads coated with mAb to CD56, MHC class II and CD8 Ags (Dynabeads 450; Dynal) [25]. The purity of $CD4^+$ T cells was more than 98% as assessed by FACS analyses. The purified responder cells (1×10^5 per well) were plated in 96-well round-bottom tissue culture plates and MØ were added to give the indicated MØ:$CD4^+$ T cell ratio. Supernatants of MØ-T cell co-cultures were collected on day 4 and the concentration of cytokines was determined.

2.4. Cytokine production

Levels of the following cytokines were measured; IFN-γ produced by $CD4^+$ T cells, IL-10, IL-1β, TNFα and IL-12p40 produced by MØ stimulated for 24 h with *M. leprae*. The concentrations of these cytokines were quantified using the enzyme assay kits, Opt EIA Human ELISA Set (BD PharMingen International).

2.5. Statistical analysis

Student's *t*-test was applied to determine the statistical differences.

3. Results

3.1. Characteristics of MØ differentiated from monocytes using GM-CSF

MØ were differentiated from monocytes using either GM-CSF (GM-MØ) or M-CSF (M-MØ). To characterize these two types of MØ, surface markers expressed on GM-MØ and M-MØ were analyzed using the monocytes obtained from the same donor by flow cytometry (Fig. 1). MHC class I (HLA-ABC) and class II (HLA-DR) Ags were similarly expressed on GM-MØ and M-MØ, but the expression of CD14 Ag was significantly reduced in GM-MØ. While the expression level of TLR2, CD209, CD40 and TLR4 Ags was not different between GM-MØ and M-MØ, the expression of CD86 was significantly higher on GM-MØ than M-MØ. Then, we examined the phagocytic capacity of GM-MØ and M-MØ by using BCG expressing GFP (GFP-BCG), since *M. leprae* cannot be cultured *in vitro* or express GFP. The percentage of MØ expressing GFP after co-culture of MØ with GFP-BCG was similar between GM-MØ and M-MØ (Fig. 2). These results indicate that GM-MØ and M-MØ differed in the expression of some surface markers, but they similarly phagocytosed the mycobacteria.

3.2. Effect of M. leprae infection to GM-MØ on the T cell-stimulating activity

Since *M. leprae* is an intracellular parasitic bacterium and is hardly digested with lysosomal enzyme in MØ unless MØ are activated [26], we analyzed the T cell-stimulating activity of *M. leprae*-infected GM-MØ and M-MØ (Table 1). When M-MØ were infected with up to MOI 80 of *M. leprae* and treated with IFN-γ and CD40L, they did not stimulate $CD4^+$ T cells to secrete a significant dose of IFN-γ. In contrast to M-MØ, when *M. leprae*-infected, IFN-γ- and CD40L-treated GM-MØ were used as Ag-presenting cells (APC), T cells produced significant levels of IFN-γ in a manner dependent on the dose of *M. leprae*. Since GM-MØ express CD40, and are activated by IFN-γ, we examined the effect of treatment with IFN-γ and CD40L on the T cell-stimulating activity of *M. leprae*-infected GM-MØ (Table 2). While IFN-γ production from $CD4^+$ T cells was not significantly induced by GM-MØ untreated or treated with either IFN-γ or CD40L, the cytokine production was significantly enhanced by the treatment of GM-MØ with

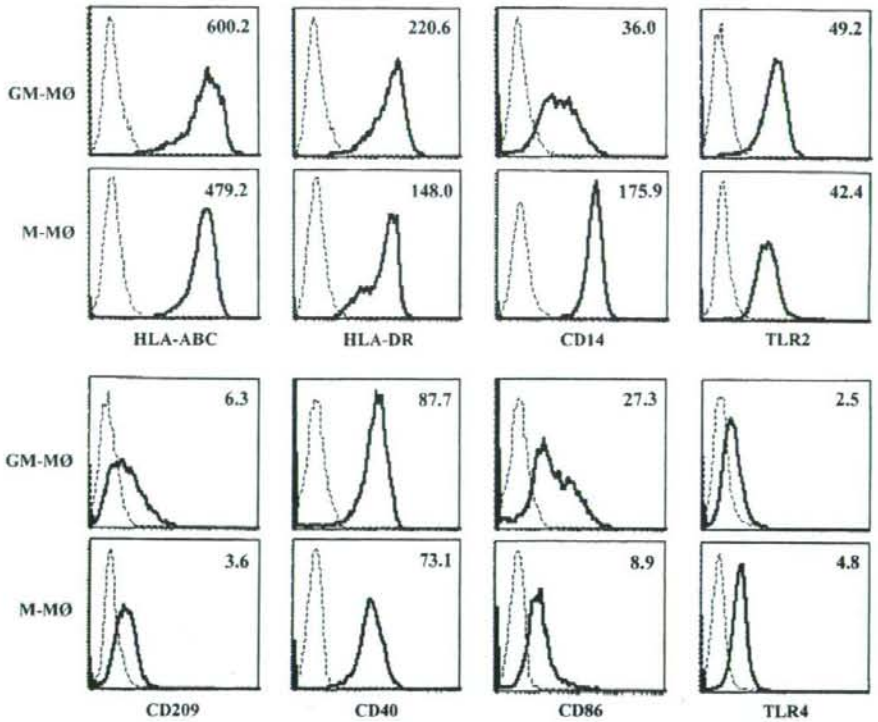

Fig. 1. Phenotype of GM-MØ and M-MØ differentiated from monocytes. Plastic adherent monocytes were differentiated into MØ by 3 days culture with either rGM-CSF or rM-CSF. Dashed lines, isotype-matched control IgG; solid lines, mAb staining. The number represents the difference in mean fluorescence intensity between dashed and solid lines. Representatives of three independent experiments are shown.

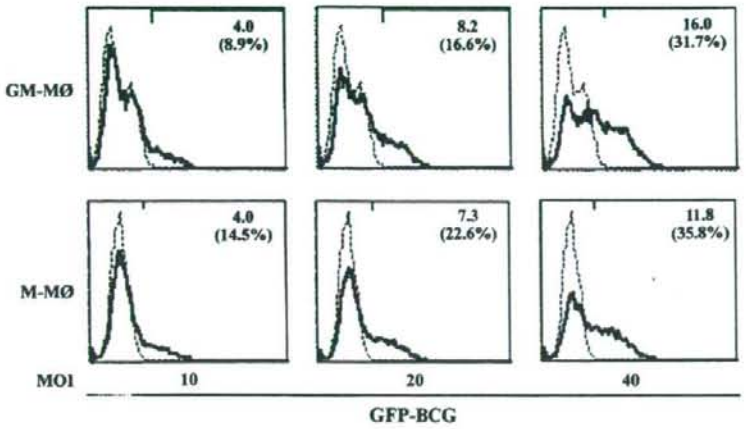

Fig. 2. Phagocytic activity of GM-MØ and M-MØ. Plastic adherent monocytes were differentiated into MØ by 3 days culture with either rGM-CSF or rM-CSF. For analysis of the phagocytic activity of MØ, GM-MØ and M-MØ were pulsed with BCG expressing GFP and assessed on day 4 of culture. Dashed lines: unpulsed cells; solid lines, GFP-BCG pulsed cells. The number represents the difference in mean fluorescence intensity between the dashed and solid lines. The number in parenthesis indicates the percent GFP-positive cell number. Representatives of three independent experiments are shown.

both IFN-γ and CD40L. Then, we compared the T cell-stimulating activity of live and heat-killed *M. leprae* (Table 3). Both forms of *M. leprae* stimulated $CD4^+$ T cells when pulsed to GM-MØ, but the heat-killed *M. leprae* more efficiently induced T cell activation than live bacteria. When we examined the effect of heat-killed *M. leprae* on M-MØ, they did not stimulate $CD4^+$ T cells significantly, even when IFN-γ and CD40L were administered (data not shown). Also note that, when GM-MØ and monocyte-derived DC were compared in terms of their T cell-stimulating activity, GM-MØ were less efficient in this respect (data not shown).

3.3. Factors associated with the enhancement of the T cell-stimulating activity of GM-MØ

Various factors may be responsible for enhancing the T cell-stimulating activity of APC. When we examined the expression of APC associated molecules on *M. leprae*-infected MØ (Fig. 3), the expression of HLA-DR and CD86 on GM-MØ was higher than on M-MØ, although there was no significant difference in the expression of HLA-ABC between GM-MØ and M-MØ. The cytokines produced from APC should also be considered to be another important factor that should be monitored and MØ produce a variety of cytokines, including IL-10, IL-1β, TNFα and IL-12 [6,11,27]. IL-10 was efficiently produced from M-MØ by stimulation with *M. leprae*, but it was hardly produced from GM-MØ (Fig. 4a). When macrophages were differentiated by using both GM-CSF and M-CSF, the function of GM-CSF was dominant and, the production of IL-10 was suppressed (Fig. 4a). Similarly to the production of IL-10, IL-1β was more efficiently produced from M-MØ than GM-MØ (Fig. 4b). In contrast, TNFα, which is important for granuloma formation, was more efficiently produced from GM-MØ (Fig. 4c). However, there was no significant difference in the production of IL-12p40 between GM-MØ and M-MØ (Fig. 4d). Finally, we assessed whether *M. leprae*-infected GM-MØ expressed dominant antigenic molecules of *M. leprae* on the surface (Fig. 5). To this end, we examined the expression of MMP-II on GM-MØ and M-MØ. No apparent expression of

Table 1
T cell-stimulating activity of *M. leprae*-infected GM-MØ and M-MØ[a]

Stimulator of $CD4^+$ T cells	*M. leprae* infection of macrophages (MOI)	IFN-γ (pg/ml) production by $CD4^+$ T cells after stimulation with macrophages at ratio (T:MØ)		
		2:1	4:1	8:1
GM-MØ	0	$0.6 \pm 0.2^{*,\dagger}$	$0.5 \pm 0.1^{\dagger,\S}$	$1.4 \pm 0.2^{\P,\|}$
	40	$38.1 \pm 3.8^{*}$	$34.2 \pm 2.3^{\ddagger}$	$23.4 \pm 3.8^{\P}$
	80	$230.7 \pm 21.4^{\dagger}$	$120.5 \pm 16.9^{\S}$	$74.7 \pm 6.8^{\|}$
M-MØ	0	0.9 ± 0.1	3.1 ± 1.2	13.9 ± 2.2
	40	0.9 ± 0.1	2.6 ± 1.3	12.2 ± 3.1
	80	11.8 ± 0.3	17.5 ± 2.1	12.2 ± 2.9

$^{*}p < 0.005$; $^{\dagger}p < 0.005$; $^{\ddagger}p < 0.01$; $^{\S}p < 0.01$; $^{\P}p < 0.01$; $^{\|}p < 0.005$.

[a] $CD4^+$ T cells (1×10^5/well) were stimulated for 4 days with autologous GM-MØ or M-MØ at the indicated dose of macrophage. GM-MØ or M-MØ were pulsed with *M. leprae* and IFN-γ (100 IU/ml) on day 3, treated with CD40L (1 μg/ml) on day 4, and were used as APC on day 5. Representatives of three separate experiments are shown. Assays were done in triplicate, and results are expressed as mean ± SD. Groups with identical symbols were compared using Student's *t*-test.

Table 2
Contribution of IFN-γ and CD40L on T cell-stimulating activity of GM-MØ[a]

M. Leprae infection of GM-MØ (MOI: 80)	Treatment of *M. leprae*-infected GM-MØ with		IFN-γ (pg/ml) production by $CD4^+$ T cells after stimulation with GM-MØ at ratio (T:MØ)		
	IFN-γ (100 IU/ml)	CD40L (1.0 μg/ml)	2:1	4:1	8:1
−	+	+	2.3 ± 0.3	0.1 ± 0.2	0.8 ± 0.5
+	−	−	4.0 ± 1.1*	5.5 ± 1.9[§]	6.0 ± 2.1[#]
+	−	+	21.4 ± 3.1[†]	22.7 ± 4.0[¶]	14.8 ± 2.2**
+	+	−	20.3 ± 1.7[‡]	15.9 ± 1.3[‖]	10.7 ± 2.3[††]
+	+	+	226.1 ± 20.9*[,†,‡]	107.8 ± 13.7[§,¶,‖]	94.8 ± 9 [*,**,#,††]

*$p < 0.005$; [†]$p < 0.005$; [‡]$p < 0.005$; [§]$p < 0.005$; [¶]$p < 0.005$; [‖]$p < 0.01$; [#]$p < 0.005$; **$p < 0.005$; [††]$p < 0.005$.

[a] $CD4^+$ T cells (1×10^5/well) were stimulated for 4 days with autologous GM-MØ at the indicated dose of macrophage. GM-MØ were pulsed with *M. leprae* and IFN-γ (100 IU/ml) on day 3, treated with CD40L (1 μg/ml) on day 4, and were used as APC on day 5. Representatives of three separate experiments are shown. Assays were done in triplicate, and the results are expressed as the mean ± SD. Groups with identical symbols were compared using Student's *t*-test.

MMP-II was observed on M-MØ, but, on GM-MØ, significant expression of MMP-II was induced. The expression was dependent on the dose of *M. leprae* (Fig. 5). However, the MMP-II expression on *M. leprae*-infected GM-MØ required both IFN-γ and CD40L, and apparent expression was not induced by sole treatment of macrophages with either IFN-γ or CD40L (data not shown).

4. Discussion

In order to avoid the intracellular multiplication and intercellular spread of *M. leprae*, the activation of adaptive immunity, especially of IFN-γ-producing type 1 T cells, plays an important role [5,6]. In fact, paucibacillary (tuberculoid) leprosy patients activate $CD4^+$ T cells through DC, although the bacteria cannot be eliminated completely [8,28]. The *M. leprae*-infected DC digest the bacteria and express dominant antigenic molecules for the efficient IFN-γ production from T cells [9]. In contrast, multibacillary (lepromatous) leprosy patients retain a large number of *M. leprae* in their MØ, and concordantly induce reduced levels or completely lack the ability to effectively stimulate T cells [11,12]. Since tissue resident MØ are heterogenous with regard to functional aspects [17,29], we assessed two different types of MØ: GM-MØ and M-MØ, and found that GM-MØ, but not M-MØ, stimulated T cells. GM-MØ were generated from monocytes using cytokine GM-CSF whilst M-MØ were produced using M-CSF. Although there were some differences in the expression levels of MHC class I, II, CD14 and CD209 Ags on GM-MØ and M-MØ, both forms were equally susceptible to mycobacteria as far as phagocytosis of BCG-GFP was examined. However, there was a striking difference between *M. leprae*-infected GM-MØ and M-MØ in the expression of antigenic molecules; only GM-MØ expressed MMP-II, which is one of the dominant antigenic molecules capable of stimulating T cells in *M. leprae*-infected individuals. The induction of MMP-II expression on GM-MØ requires not only GM-CSF, but also the co-stimulation of MØ with IFN-γ and CD40L. In case of *M. leprae*-infected DC, the phagosomal bacteria could be processed by lysosomal enzymes, and MMP-II expression was observed on DC [9]. The MMP-II expression observed on GM-MØ may indicate that at least some intracellular *M. leprae* were processed. However, the processing of *M. leprae* by GM-MØ still seemed partial, since the heat-killed *M. leprae* induced T cell activation more vigorously than live bacteria, and *M. leprae*-infected DC stimulated T cells more efficiently than GM-MØ, although other factors, such as an induction of IL-12, cannot be ruled out completely. The cell wall architecture including surface-exposed molecules, of heat-killed mycobacteria is globally altered [29,30], resulting in the exudation of some soluble antigenic molecules which may be feasibly digested in macrophages (unpublished observation). Therefore, T cells are more efficiently activated by heat-killed bacteria than by live bacteria.

Table 3
Comparison of T cell-stimulating activity of live and heat-inactivated *M. leprae*[a]

M. leprae pulsed on GM-MØ (MOI)	IFN-γ (pg/ml) production by $CD4^+$ T cells after stimulation with GM-MØ at ratio (T:MØ)		
	2:1	4:1	8:1
None	2.3 ± 1.1	2.1 ± 1.2	2.4 ± 0.9
HK (40)	406.5 ± 49.3*	157.3 ± 20.1[‡]	75.4 ± 6.8[¶]
HK (80)	399.8 ± 33.2[†]	187.7 ± 17.8[§]	106.9 ± 11.2[‖]
Live (40)	101.5 ± 8.8*	30.2 ± 4.6[‡]	3.2 ± 1.9[¶]
Live (80)	152.0 ± 12.7[†]	82.9 ± 7.4[§]	32.7 ± 2.8[‖]

*$p < 0.01$; [†]$p < 0.005$; [‡]$p < 0.005$; [§]$p < 0.005$; [¶]$p < 0.005$; [‖]$p < 0.005$.

[a] $CD4^+$ T cells (1×10^5/well) were stimulated for 4 days with autologous GM-MØ at the indicated dose of macrophage. GM-MØ were pulsed with either heat-killed (HK) or live *M. leprae* and IFN-γ (100 IU/ml) on day 3, treated with CD40L (1 μg/ml) on day 4, and were used as APC on day 5. Representatives of three separate experiments are shown. Assays were done in triplicate, and the results are expressed as the mean ± SD. Groups with identical symbols were compared using Student's *t*-test.

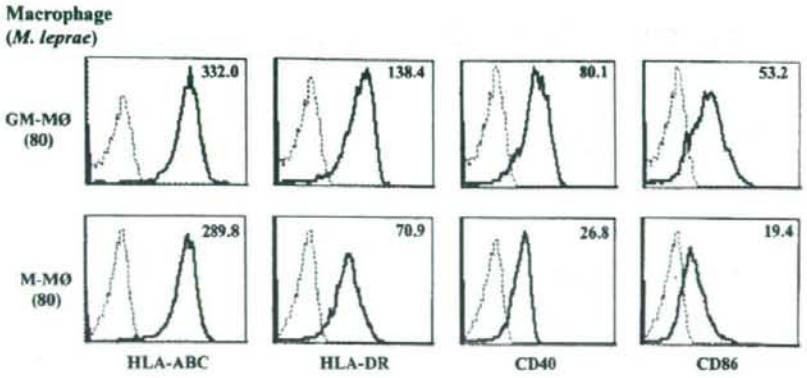

Fig. 3. Phenotype of *M. leprae*-infected GM-MØ and M-MØ. GM-MØ and M-MØ differentiated from monocytes by 3 days culture with rGM-CSF or rM-CSF were infected with *M. leprae*, treated with IFN-γ (100 IU/ml) on day 3, and further treated with CD40L (1 μg/ml) on day 4 of culture. On day 5, the phenotype of GM-MØ and M-MØ was analyzed. Dashed lines, isotype-matched control IgG; solid lines, mAb staining. The number represents the difference in mean fluorescence intensity between dashed and solid lines. Representatives of three independent experiments are shown.

Ottenhoff et al. have also reported that GM-CSF up-regulates the T cell-stimulating activity of MØ, but not M-CSF, and mycobacteria-infected GM-MØ promoted the type 1 cell-mediated immunity against pathogens [31]. Our observations are in line with their data and provide ways to enhance the cell-mediated immunity, especially in cases progressing towards lepromatous leprosy. To facilitate the T cell activation and MMP-II expression, it was required to use

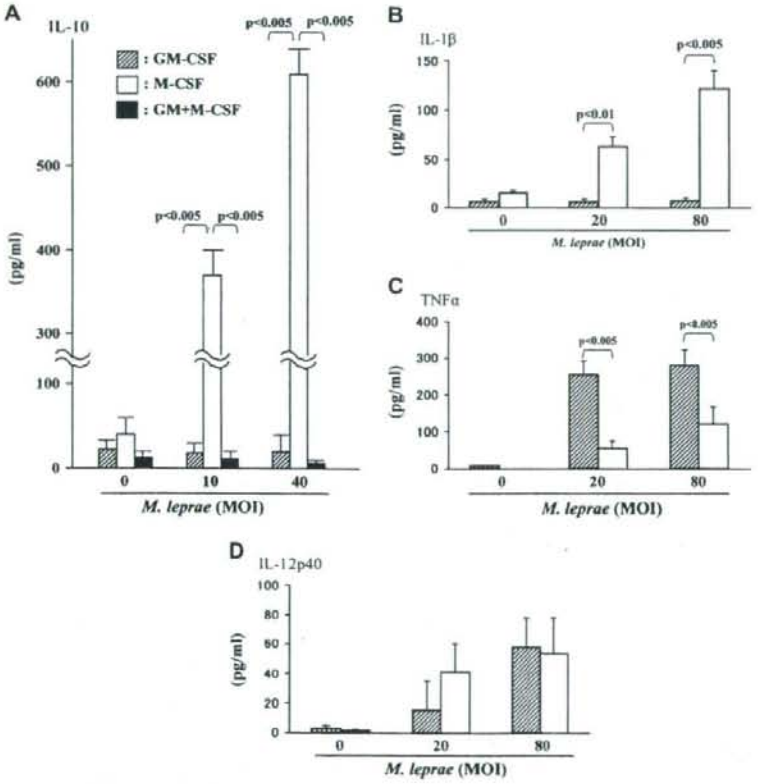

Fig. 4. Cytokine production from GM-MØ and M-MØ. MØ were differentiated by 3 days culture with rGM-CSF, rM-CSF or rGM-CSF + rM-CSF, and were stimulated with *M. leprae* for 24 h. The cytokines: (a) IL-10; (b) IL-1β; (c) TNFα; and (d) IL-12p40 were measured by ELISA. Representatives of three independent experiments are shown.

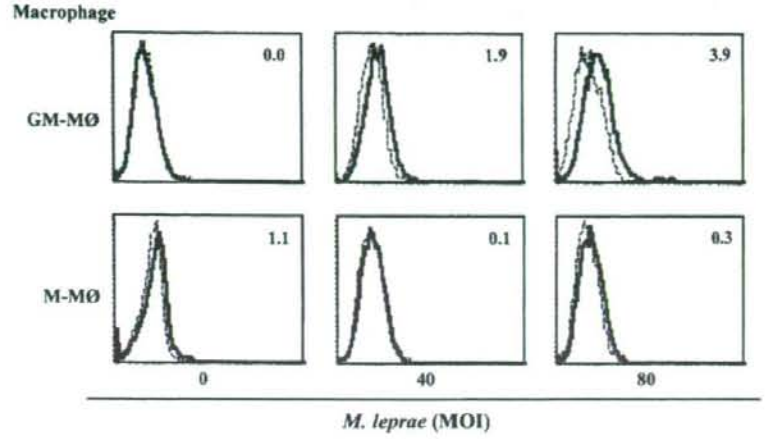

Fig. 5. Expression of MMP-II on the surface of GM-MØ and M-MØ. GM-MØ and M-MØ were differentiated from monocytes by 3 days culture with either rGM-CSF or rM-CSF, respectively. These macrophages were infected with an indicated dose of *M. leprae* and treated with IFN-γ (100 IU/ml) on day 3 of monocyte culture, further treated with CD40L (1 μg/ml) on day 4, and were analyzed for MMP-II expression on day 5. Dashed lines, control IgM; solid lines, MMP-II mAb staining. The number represents the difference in mean fluorescence intensity between dashed and solid lines. Representatives of three independent experiments are shown.

both IFN-γ and CD40L, in addition to the lineage-determining cytokine GM-CSF. IFN-γ and CD40L are probably required to compensate for the lower antigenic characteristics of *M. leprae* [24]. Studies using other mycobacteria, such as *M. bovis* BCG, may provide further useful information. Although IFN-γ is known to activate MØ for bacterial digestion and to induce IL-12p35 gene transcription [26,31], it remains to be determined if CD40L treatment on GM-MØ furthers the intracellular processing of phagosomal bacteria or whether conditioning of GM-MØ through CD40-CD40L interaction, such as in DC [32], is required for T cell stimulation. In addition to MMP-II expression, there were some differences in the phenotypic features of *M. leprae*-infected GM-MØ and M-MØ. A higher level of HLA-DR and CD86 Ags was expressed on the GM-MØ infected with *M. leprae* and co-stimulated, than on similarly treated M-MØ. The mechanism, leading to the enhanced Ag expression, especially of Ag processing by IFN-γ, has not been clearly demonstrated and remains to be elucidated, but GM-CSF, IFN-γ and CD40L seem to at least partially co-ordinate and induce the higher expression of HLA-DR and CD86. These phenotypic differences between *M. leprae*-infected GM-MØ and M-MØ again contribute to the differences in T cell stimulatory activity.

Another peculiar difference observed between the two types of MØ, GM-MØ and M-MØ, was the cytokines that they induced. IL-10 suppresses DC-dependent as well as DC-independent T cell activation [14,15,33], and creates a situation in which *M. leprae* can feasibly parasitize in the cells. While M-MØ secreted a large amount of IL-10, GM-MØ completely lacked in the production of cytokine upon stimulation with *M. leprae* (Fig. 4) or lipopolysaccharide (data not shown). Furthermore, the presence of GM-CSF diminished the IL-10 production from M-MØ by *M. leprae*. Thus, treatment of monocytes with GM-CSF can wipe off the favorable conditions for *M. leprae* survival. On the other hand, GM-MØ produced a higher level of TNFα than M-MØ. TNFα plays an important role in the granuloma formation, and TNFα is an important mediator of host defense activity in MØ, in mycobacterial lesions [34,35]. The treatment of monocyte with GM-CSF would be beneficial for MØ-mediated host defense in this respect. These observations were consistent with the previous findings that IL-10-deficient mice display increased anti-mycobacterial immunity with concordant higher levels of TNFα and a lower bacterial burden [36]. Our previous studies show that T cells from lepromatous leprosy can mount a significant production of IFN-γ by appropriate stimulation [10], therefore, the present studies may provide useful information for the development of immunotherapeutic tools, such as endogenous or exogenous treatment of macrophages with GM-CSF, and thus prevent the dissemination of *M. leprae*.

In this study, we analyzed the two types of MØ with regard to T cell-stimulating activity, and found that GM-CSF and co-stimulators enhance the host defense activity of *M. leprae*-infected MØ.

Acknowledgments

We acknowledge the contribution of Ms. N. Makino in the preparation of this manuscript. We also thank Ms. Y. Harada for technical support, and the Japanese Red Cross Society for kindly providing PBMC from healthy donors.

This work was supported in part by a Grant-in-Aid for Research on Emerging and Re-emerging Infectious Diseases and by a Grant-in-Aid for Research on HIV/AIDS from the Ministry of Health, Labour and Welfare of Japan.

References

[1] G.L. Stoner, Importance of the neural predilection of *Mycobacterium leprae* in leprosy, Lancet 2 (1979) 994–996.

[2] C.K. Job, Nerve damage in leprosy, Int. J. Lepr. Other Mycobact. Dis. 57 (1989) 532–539.
[3] S.N.C. Wemambu, J.L. Turk, M.F.R. Waters, R.J.W. Rees, *Erythema nodosum leprosum*: a clinical manifestation of the Arthus phenomenon, Lancet 2 (1969) 933–935.
[4] S. Verghese, D.G. Healey, J. Curtis, J.L. Turk, Accessory cell function of dendritic cells from lymph nodes containing *Mycobacterium leprae* induced granulomas, Int. Arch. Allergy Appl. Immunol. 87 (1988) 392–399.
[5] P. Salgame, J.S. Abrams, C. Clayberger, H. Goldstein, J. Convit, R.L. Modlin, B.R. Bloom, Differing lymphokine profiles of functional subsets of human CD4 and CD8 T cell clones, Science 254 (1991) 279–282.
[6] M. Yamamura, K. Uyemura, R.J. Deans, K. Weinberg, T.H. Rea, B.R. Bloom, R.L. Modlin, Defining protective responses to pathogens: cytokine profiles in leprosy lesions, Science 254 (1991) 277–279.
[7] P.S. Yamauchi, J.R. Bleharski, K. Uyemura, J. Kim, P.A. Sieling, A. Miller, H. Brightbill, K. Schlienger, T.H. Rea, R.L. Modlin, A role for CD40–CD40 ligand interactions in the generation of type 1 cytokine responses in human leprosy, J. Immunol. 165 (2000) 1506–1512.
[8] S.R. Krutzik, B. Tan, H. Li, M.T. Ochoa, P.T. Liu, S.E. Sharfstein, T.G. Graeber, P.A. Sieling, Y.-J. Liu, T.H. Rea, B.R. Bloom, R.L. Modlin, TLR activation triggers the rapid differentiation of monocytes into macrophages and dendritic cells, Nat. Med. 11 (2005) 653–660.
[9] Y. Maeda, T. Mukai, J. Spencer, M. Makino, Identification of an immunomodulating agent from *Mycobacterium leprae*, Infect. Immun. 73 (2005) 2744–2750.
[10] M. Makino, Y. Maeda, N. Ishii, Immunostimulatory activity of major membrane protein-II from *Mycobacterium leprae*, Cell. Immunol. 233 (2005) 53–60.
[11] D.S. Ridley, W.H. Jopling, Classification of leprosy according to immunity. A five-group system, Int. J. Lepr. Other Mycobact. Dis. 34 (1966) 255–273.
[12] D.A. Hagge, N.A. Ray, J.L. Krahenbuhl, L.B. Adams, An *in vitro* model for the lepromatous leprosy granuloma: fate of *Mycobacterium leprae* from target macrophages after interaction with normal and activated effector macrophages, J. Immunol. 172 (2004) 7771–7779.
[13] C. Frehel, N. Rastogi, *Mycobacterium leprae* surface components intervene in the early phagosome–lysosome fusion inhibition event, Infect. Immun. 55 (1987) 2916–2921.
[14] H. Jonuleit, E. Schmitt, K. Steinbrink, A.H. Enk, Dendritic cells as a tool to induce anergic and regulatory T cells, Trends Immunol. 22 (2001) 394–400.
[15] A. Granelli-Piperno, A. Golebiowska, C. Trumpfheller, F.P. Siegal, R.M. Steinman, HIV-1-infected monocyte-derived dendritic cells do not undergo maturation but can elicit IL-10 production and T cell regulation, Proc. Natl. Acad. Sci. U.S.A. 101 (2004) 7669–7674.
[16] K. Nakata, K.S. Akagawa, M. Fukayama, Y. Hayashi, M. Kadokura, T. Tokunaga, Granulocyte-macrophage colony-stimulating factor promotes the proliferation of human alveolar macrophages *in vitro*, J. Immunol. 147 (1991) 1266–1272.
[17] K.S. Akagawa, Functional heterogeneity of colony-stimulating factor-induced human monocyte-derived macrophages, Int. J. Hematol. 76 (2002) 27–34.
[18] M.U. Martin, H. Wesche, Summary and comparison of the signaling mechanisms of the Toll/interleukin-1 receptor family, Biochim. Biophys. Acta 1592 (2002) 265–280.
[19] M. Makino, M. Baba, A cryopreservation method of human peripheral blood mononuclear cells for efficient production of dendritic cells, Scand. J. Immunol. 45 (1997) 618–622.
[20] G.J. Randolph, K. Inaba, D.F. Robbiani, R.M. Steinman, W.A. Muller, Differentiation of phagocytic monocytes into lymph node dendritic cells in vivo, Immunity 11 (1999) 753–761.
[21] M. Makino, S. Shimokubo, S. Wakamatsu, S. Izumo, M. Baba, The role of human T-lymphotropic virus type 1 (HTLV-1)-infected dendritic cells in the development of HTLV-1-associated myelopathy/tropical spastic paraparesis, J. Virol. 73 (1999) 4575–4581.
[22] R.D. McDermott-Lancaster, T. Ito, K. Kohsaka, C.C. Guelpa-Lauras, J.H. Grosset, Multiplication of *Mycobacterium leprae* in the nude mouse, and some applications of nude mice to experimental leprosy, Int. J. Lepr. Other Mycobact. Dis. 55 (1987) 889–895.
[23] C.K. Stover, V.F. de la Cruz, T.R. Fuerst, J.E. Burlein, L.A. Benson, L.T. Bennett, G.P. Bansal, J.F. Young, M.H. Lee, G.F. Hatfull, S.B. Snapper, R.G. Barletta, W.R. Jacobs Jr., B.R. Bloom, New use of BCG for recombinant vaccines, Nature 351 (1991) 456–460.
[24] K. Hashimoto, Y. Maeda, H. Kimura, K. Suzuki, A. Masuda, M. Matsuoka, M. Makino, *Mycobacterium leprae* infection in monocyte-derived dendritic cells and its influence on antigen presenting function, Infect. Immun. 70 (2002) 5167–5176.
[25] S. Wakamatsu, M. Makino, C. Tei, M. Baba, Monocyte-driven activation-induced apoptotic cell death of human T-lymphotropic virus type I-infected T cells, J. Immunol. 163 (1999) 3914–3919.
[26] H. Kimura, Y. Maeda, F. Takeshita, L.E. Takaoka, M. Matsuoka, M. Makino, Upregulation of T-cell-stimulating activity of mycobacteria-infected macrophages, Scand. J. Immunol. 60 (2004) 278–286.
[27] M.M. Stefani, C.M. Martelli, T.P. Gillis, J.L. Krahenbuhl, Brazilian Leprosy Study Group, In situ type 1 cytokine gene expression and mechanisms associated with early leprosy progression, J. Infect. Dis. 188 (2003) 1024–1031.
[28] P.A. Sieling, D. Jullien, M. Dahlem, T.F. Tedder, T.H. Rea, R.L. Modlin, S.A. Porcelli, CD1 expression by dendritic cells in human leprosy lesions: correlation with effective host immunity, J. Immunol. 162 (1999) 1851–1858.
[29] P.B. Kang, A.K. Azad, J.B. Torrelles, T.M. Kaufman, A. Beharka, E. Tibesar, L.E. Desjardin, L.S. Schlesinger, The human macrophage mannose receptor directs *Mycobacterium tuberculosis* lipoarabinomannan-mediated phagosome biogenesis, J. Exp. Med. 202 (2005) 987–999.
[30] I. Vergne, J. Chua, H.H. Lee, M. Lucas, J. Belisle, V. Deretic, Mechanism of phagolysosome biogenesis block by viable *Mycobacterium tuberculosis*, Proc. Natl. Acad. Sci. U.S.A. 102 (2005) 4033–4038.
[31] F.A. Verreck, T. de Boer, D.M. Langenberg, M.A. Hoeve, M. Kramer, E. Vaisberg, R. Kastelein, A. Kolk, R. de Waal-Malefyt, T.H. Ottenhoff, Human IL-23-producing type 1 macrophages promote but IL-10-producing type 2 macrophages subvert immunity to (myco)bacteria, Proc. Natl. Acad. Sci. U.S.A. 101 (2004) 4560–4565.
[32] C. Caux, C. Massacrier, B. Vanbervliet, B. Dubois, C. Van Kooten, I. Durand, J. Banchereau, Activation of human dendritic cells through CD40 cross-linking, J. Exp. Med. 180 (1994) 1263–1272.
[33] K. Mochida-Nishimura, K.S. Akagawa, E.A. Rich, Interleukin-10 contributes development of macrophage suppressor activities by macrophage colony-stimulating factor, but not by granulocyte-macrophage colony-stimulating factor, Cell. Immunol. 214 (2001) 81–88.
[34] J.H. Davis, H. Clay, J.L. Lewis, N. Ghori, P. Herbomel, L. Ramakrishnan, Real-time visualization of mycobacterium–macrophage interactions leading to initiation of granuloma formation in zebrafish embryos, Immunity 17 (2002) 693–702.
[35] E. Giacomini, E. Iona, L. Ferroni, M. Miettinen, L. Fattorini, G. Orefici, I. Julkunen, E.M. Coccia, Infection of human macrophages and dendritic cells with *Mycobacterium tuberculosis* induces a differential cytokine gene expression that modulates T cell response, J. Immunol. 166 (2001) 7033–7041.
[36] P.J. Murray, R.A. Young, Increased antimycobacterial immunity in interleukin-10-deficient mice, Infect. Immun. 67 (1999) 3087–3095.

JOURNAL OF BACTERIOLOGY, Nov. 2007, p. 8241–8249
0021-9193/07/$08.00+0 doi:10.1128/JB.00550-07

Vol. 189, No. 22

Control of Cell Wall Assembly by a Histone-Like Protein in Mycobacteria[▽]

Tomoya Katsube,[1,2] Sohkichi Matsumoto,[1]* Masaki Takatsuka,[1,2] Megumi Okuyama,[1] Yuriko Ozeki,[3] Mariko Naito,[4] Yukiko Nishiuchi,[1] Nagatoshi Fujiwara,[1] Mamiko Yoshimura,[1] Takafumi Tsuboi,[5] Motomi Torii,[6] Nobuhide Oshitani,[2] Tetsuo Arakawa,[2] and Kazuo Kobayashi[7]

Department of Host Defense[1] and Department of Gastroenterology,[2] Osaka City University Graduate School of Medicine, 1-4-3 Asahi-machi, Abeno-ku, Osaka 545-8585, Japan; Sonoda Women's University, 7-29-1 Minamitsukaguchi-cho, Amagasaki, Hyogo, Japan[3]; Division of Microbiology and Oral Infection, Department of Molecular Microbiology and Immunology, Nagasaki University Graduate School of Biomedical Sciences, 1-7-1 Sakamoto, Nagasaki 852-8588, Japan[4]; Cell-Free Science and Technology Research Center and Venture Business Laboratory, Ehime University, 3 Bunkyo-cho, Matsuyama, Ehime 790-8577, Japan[5]; Department of Molecular Parasitology, Ehime University Graduate School of Medicine, Toon, Ehime 791-0295, Japan[6]; and Department of Immunology, National Institute of Infectious Diseases, Toyama 1-23-1, Shinjuku-ku, Tokyo 162-8640, Japan[7]

Received 11 April 2007/Accepted 1 September 2007

Bacteria coordinate assembly of the cell wall as well as synthesis of cellular components depending on the growth state. The mycobacterial cell wall is dominated by mycolic acids covalently linked to sugars, such as trehalose and arabinose, and is critical for pathogenesis of mycobacteria. Transfer of mycolic acids to sugars is necessary for cell wall biogenesis and is mediated by mycolyltransferases, which have been previously identified as three antigen 85 (Ag85) complex proteins. However, the regulation mechanism which links cell wall biogenesis and the growth state has not been elucidated. Here we found that a histone-like protein has a dual concentration-dependent regulatory effect on mycolyltransferase functions of the Ag85 complex through direct binding to both the Ag85 complex and the substrate, trehalose-6-monomycolate, in the cell wall. A histone-like protein-deficient *Mycobacterium smegmatis* strain has an unusual crenellated cell wall structure and exhibits impaired cessation of glycolipid biosynthesis in the growth-retarded phase. Furthermore, we found that artificial alteration of the amount of the extracellular histone-like protein and the Ag85 complex changes the growth rate of mycobacteria, perhaps due to impaired down-regulation of glycolipid biosynthesis. Our results demonstrate novel regulation of cell wall assembly which has an impact on bacterial growth.

Bacteria organize biogenesis of the cell wall as well as synthesis of cellular components depending on the growth state. However, factors linking the growth state and cell wall biogenesis have not been identified.

Mycobacterium tuberculosis is a top killer among bacterial pathogens and is responsible for 2 million deaths annually (6). *M. tuberculosis* can be quiescent in host cells for a long period of time, growing very slowly or present in a dormant state without multiplication, and it latently infects one-third of the world's human population (22, 43). In 5 to 10% of infected hosts the bacterium reactivates and causes progressive disease during their lifetimes. Most cases of active tuberculosis do not result from the initial infection but instead represent reactivation of previously implanted bacteria (22, 43).

The cell wall is critical for long-term persistence of *M. tuberculosis* in the hostile environment in the host cells and for progression of tuberculosis (3, 7). Mycobacteria are gram-positive bacilli, but the cell wall structures are different from those of other gram-positive bacteria. Approximately one-half of the cell wall mass is comprised of large (C_{70} to C_{90}) branched-chain fatty acids called mycolic acids. Mycolic acids are distributed in acid-fast positive bacteria, such as *Mycobacterium*, *Corynebacterium*, *Rhodococcus*, and *Nocardia*, although mycobacterial mycolic acids are the longest mycolic acids and have the largest side chains (C_{20} to C_{24}). The cell wall outer layer is composed of extractable glycolipids containing mycolic acids, such as trehalose-6-monomycolate (TMM) and trehalose-6,6′-dimycolate (TDM) (also called cord factor), while the inner layer is composed of mycolic acids covalently linked to the distal portion of the arabinogalactan (AG) moiety (7). TMM- or TDM-derived mycolic acids are transferred to other TMM to synthesize TDM and also to peptidoglycan-linked AG to construct the inner layer of the envelope. Antigen 85 (Ag85) complex proteins (Ag85A, Ag85B, and Ag85C) are mycolyltransferases and catalyze transfer of mycolic acids to free trehalose, TMM, and TDM (4). Ag85 complex proteins are also believed to catalyze the transfer of mycolic acids from TMM or TDM to peptidoglycan-linked AG, because inactivation of Ag85C reduced the level of AG-linked mycolic acids (16).

Regulatory proteins involved in cell wall assembly should localize in the mycobacterial cell wall. We and other groups found that a histone-like DNA-binding protein, which was designated mycobacterial DNA-binding protein 1 (MDP1), laminin-binding protein, histone-like protein (HLP), or HupB, not only localizes in the cytoplasmic space but also occurs externally or is in the mycobacterial cell wall (26, 36, 38).

* Corresponding author. Mailing address: Department of Host Defense, Osaka City University Graduate School of Medicine, 1-4-3 Asahi-machi, Abeno-ku, Osaka 545-8585, Japan. Phone: 81-6-6645-3746. Fax: 81-6-6645-3747. E-mail: sohkichi@med.osaka-cu.ac.jp.

▽ Published ahead of print on 14 September 2007.

MDP1 is mycobacterium-specific histone-like protein. *M. tuberculosis* has a single *mdp1* gene (Rv2986c, also called *hupB*) (9, 13), and the *mdp1* gene is conserved even in *Mycobacterium leprae*, which lost many genes during evolution (10). MDP1 likely plays a significant role in DNA functions in mycobacteria, as a transposon-based screen suggested that *mdp1* is essential in *M. tuberculosis* (34). However, the *mdp1* gene can be knocked out in *Mycobacterium smegmatis*, suggesting that another DNA-binding protein may compensate for loss of MDP1 in *M. smegmatis*. The *M. smegmatis* MDP1 knockout (KO) strain exhibited growth kinetics similar to those of the wild type in anaerobic culture (19) but was unable to resume growth at 10°C (37), suggesting that MDP1 plays an important role during stress responses in *M. smegmatis*.

Accumulation of MDP1 in stationary phase or under anaerobic conditions implies that MDP1 is a possible factor that participates in growth-state-dependent regulation of cell wall assembly through binding to sacchariferous components, such as glycolipids, in the cell wall. Based on this hypothesis, here we examined the physiological role of MDP1 in the cell wall.

MATERIALS AND METHODS

Extraction and purification of glycolipids. *M. tuberculosis* H37Rv and *Mycobacterium bovis* bacillus Calmette-Guérin (BCG) were cultivated on Sauton medium at 37°C. *M. smegmatis* was cultured in Luria-Bertani (LB) medium at 37°C. Bacteria were autoclaved for 10 min, disrupted ultrasonically, and then suspended in chloroform-methanol (4:1, 3:1, or 2:1, vol/vol) to extract lipids. The chloroform layer was collected and dried. TDM was first partially purified by precipitation with acetone, chloroform-methanol (2:1, vol/vol), and tetrahydrofuran-methanol (1:2, vol/vol), followed by passage through a column of silica gel (Wakogel C-200; Wako Pure Chemical, Osaka, Japan) with chloroform-methanol (4:1, vol/vol). The purity of TDM was demonstrated by a single spot on a thin-layer chromatogram. TMM was separated by preparative thin-layer chromatography (TLC) on a silica gel plate (Uniplate; 20 by 20 cm; 250 mm; Analtech, Inc., Newark, DE) using a chloroform-methanol-acetone-acetic acid (80:20:6:1, vol/vol/vol/vol) solvent system. Glycolipids were visualized with a 20% H_2SO_4 spray, followed by charring at 200°C for analytical purposes or with iodine vapor for a few minutes for preparative purposes. TMM was recovered from the plate immediately after the iodine color had disappeared by passing the plate through a small glass column with the solvent chloroform-methanol (2:1, vol/vol). Finally, TMM was purified until a single spot was obtained by repeating TLC.

Fluorescence microscopy. MDP1 was purified from BCG by using a method described previously (26). Egg white lysozyme was purchased from Wako. Bovine histone H1 was purchased from Roche Diagnostics. Proteins were labeled with 5(6)-carboxyfluorescein-*N*-hydroxysuccinimide ester (FLUOS) by using a fluorescein protein labeling kit (Roche Diagnostics) according to the manufacturer's instructions. BCG was grown in Middlebrook 7H9-ADC medium at 37°C until the optical density at 600 nm (OD_{600}) was 1.5; then it was collected by centrifugation and washed three times with phosphate-buffered saline (PBS) with 10% fetal bovine serum (FBS). FLUOS-labeled proteins, such as MDP1 (50 μg), egg white lysozyme (38 μg), and bovine histone H1 (50 μg), were added to the BCG suspension and incubated at 37°C for 30 min. BCG was washed three times with PBS with 10% FBS and then mounted on a microscope slide and viewed with a confocal scanning laser microscope (LSM510; Carl Zeiss).

MAb preparation. Ten micrograms of MDP1 and 10 ng of *M. tuberculosis* DNA were mixed in PBS, emulsified in Freund's incomplete adjuvant, and injected into BALB/c mice subcutaneously (24). Two weeks later, the mice were boosted in the same way; after an additional 2 weeks, the mice were again boosted by injection of 10 μg of MDP1 in PBS into the tail vein. Three days after the final boost, mice were sacrificed and splenocytes were obtained. A monoclonal antibody (MAb) was prepared essentially as described by Harlow and Lane (15) and was screened by an enzyme-linked immunosorbent assay (ELISA) as described below. After an initial screening, several hybridoma cell lines were cloned by two rounds of limiting dilution. A selected subclone was expanded for freezing and for ascites production in pristane-primed mice. The subclass of the hybridoma subclone was determined with a mouse MAb isotyping kit (Amersham). Immunoglobulins (Ig) were purified from ascites fluid by using an Ampure PA kit (Amersham).

ELISA to detect interactions between MDP1 and TDM, TMM, mycolic acids, or Ag85 complex proteins. TMM, TDM, and mycolic acid methyl esters (MAMEs) purified from *M. tuberculosis* Aoyama B were purchased from Nakarai and dissolved in *N*-hexane at a concentration of 50 μg/ml. Glycolipids were immobilized on a 96-well ELISA plate (Sumitomo, Osaka, Japan) by adding 100 μl of glycolipid solution and dried. Ag85A, Ag85B, and Ag85C derived from *M. tuberculosis* H37Rv and bovine serum albumin (BSA) were immobilized on the 96-well ELISA plate (Sumitomo, Osaka, Japan) by incubation of serial twofold dilutions of the protein solutions in sodium bicarbonate buffer (pH 9.6) at 4°C overnight. MDP1 at a concentration of 1 μg/ml in PBS containing 0.05% Tween 20 (PBS-T) was added to wells and incubated for 1 h at 37°C. The wells were washed with PBS-T four times, and then MAb 3A was added. After incubation at 37°C for 1 h, the wells were washed, peroxidase-conjugated anti-mouse antibody (Dako) diluted 1:2,000 was added, and the plate was incubated for 1 h. After the wells were washed, the level of MDP1 binding was detected by color development with *o*-phenylenediamine dihydrochloride (Wako, Tokyo, Japan) and measuring the OD_{492}.

Preparation of subcellular fractions. Subcellular fractions were prepared by a method described previously (1, 27). Briefly, after BCG and *M. smegmatis* were cultured in Sauton medium and LB medium, respectively, bacteria were collected by centrifugation at 10,000 × *g* and suspended in ice-cold PBS. The bacteria were then disrupted with a Bioruptor UCD-200T sonicator (Toso), and each suspension was centrifuged at 3,000 × *g* for 5 min to remove unbroken bacteria. The supernatant was used as the total cellular fraction. The total cellular fraction was fractionated further to obtain a cell wall fraction and a non-cell-wall fraction using the following procedure. The total cellular fraction was centrifuged at 10,000 × *g* for 10 min. The pellet was rinsed with cold PBS and centrifuged again at 10,000 × *g* for 10 min. The supernatants were designated the non-cell-wall fraction. The cell wall-containing pellet was suspended again in ice-cold PBS, and then Percoll (Amersham Biosciences) was added to a concentration of 60% and mixed by vortexing. Next, the cell wall-containing fraction was centrifuged at 27,000 × *g* for 1 h to separate the cell walls from the unbroken cells completely. The cell wall band was collected and washed twice with PBS, and it was designated the cell wall fraction.

Immunoprecipitation assay. Cell walls derived from BCG as described above were precleaned by using 25 μg of mouse IgG (Chemicon International Temecula) or rabbit Ig in 100 μl of protein G-coupled Sepharose (Amersham Pharmacia Biotech), incubated at 4°C for 2 h, and centrifuged. The supernatants were colleted and incubated with 250 μg of anti-MDP1 MAb 3A, control mouse IgG, anti-Ag85 Ig, or control rabbit Ig at 4°C for 16 h, and then 300 μl of protein G-coated Sepharose was added and the preparation was incubated for 5 h at 4°C. Then the beads were washed with PBS-T three times. After washing, bead-bound proteins were eluted by boiling the preparations in 40 μl of 2× sodium dodecyl sulfate (SDS)-polyacrylamide gel electrophoresis (PAGE) sample buffer (0.125 M Tris-HCl [pH 6.8], 4% SDS, 20% glycerol, 10% mercaptoethanol). The samples were then fractionated on a 12.5% SDS-polyacrylamide gel and transferred to a polyvinylidene difluoride membrane. The membrane was then blocked for 30 min at room temperature by incubating it in PBS containing 5% skim milk. Then the membrane was probed with anti-MDP1 MAb 3A or anit-Ag85 antibodies overnight at 4°C. After probing, the membrane was washed four times with PBS-T. Next, the membrane was incubated for 4 h at room temperature with peroxidase-conjugated anti-mouse IgG or anti-rabbit IgG (Dakopatts A/S, Denmark) diluted 1:10,000. The membrane was then washed as described above, and immunoreactive bands were visualized by using an ECL Western blot detection reagent (Amersham Bioscience, Buckinghamshire, United Kingdom) according to the manufacturer's instructions.

Bead-bound glycolipids were eluted with chloroform-methanol (3:1, vol/vol). Thirty microliters of the chloroform layer was spotted on a TLC plate (HPTLC plate; 10 by 10 cm; Silica Gel 60; Merck, Darmstadt, Germany) and developed with the chloroform-methanol-acetone-acetic acid (80:20:6:1, vol/vol/vol/vol) solvent system. The TLC plate was exposed overnight to an immunoprecipitation plate (BAS-MS2025 or BAS-SR2025; Fujifilm, Japan) and visualized with the BAS system (BAS-5000). The radioactivity of separated spots was quantified by using the BAS system's software.

Analysis of mycolyltransferase activity. The mycolyltransferase catalytic reaction was analyzed by using the method developed by Belisle et al. (4). Twenty-five micrograms of TMM purified from *M. tuberculosis* H37Rv was immobilized in each glass vial, and then PBS containing 4 μl of a 1-mg/ml dithiothreitol solution and 0.5 μCi of [^{14}C]trehalose (American Radiolabeled Chemicals Inc.) were added. Two hundred micrograms of culture filtrate or 20 μg of Ag85 complex protein and various amounts of MDP1 or BSA were mixed to obtain a total

volume of 200 μl and incubated for 30 min at 37°C. Glycolipids were eluted with chloroform-methanol (2:1, vol/vol), 10 μl of the chloroform layer was spotted on a TLC plate (HPTLC plate; 10 by 10 cm; Silica Gel 60; Merck, Darmstadt, Germany), and the plate was developed with the chloroform-methanol-acetone-acetic acid (80:20:6:1, vol/vol/vol/vol) solvent system. TLC plates were analyzed by using the BAS system described above.

Construction of HLP/MDP1 complemented strain. Based on the *mdp1/hlp* nucleotide sequences, two oligonucleotide primers, forward primer 5′-GGGAA GCTTATTCGCCGCCCACCTAGT-3′ and reverse primer 5′-TAACGCACCA ACGCGAAA-3′, were purchased from Sigma Genosys. A PCR was carried out by targeting 10 ng chromosomal DNA of *M. smegmatis* MC^2155 with an automated thermal sequencer (Perkin Elmer). The samples were first denatured by heating them at 94°C for 5 min; then they were subjected to 30 cycles of 94°C for 1 min, 58°C for 1 min, and 72°C for 3 min and were finally incubated for 5 min at 72°C. An amplified 0.9-kb DNA fragment, which contained the promoter and structural gene of HLP/MDP1, was cloned into pGEM-T (Promega) utilizing a ligation kit (version 1; Takara), sequenced, excised by digestion with HindIII and NotI, and ligated to the same site of pMV306-Hyg, a one-copy integrated vector for the phage attachment site. pMV306-Hyg was provided by H. I. Boshoff (National Institutes of Health, Bethesda, MD). The resulting plasmid was introduced into an *M. smegmatis* HLP/MDP1 KO strain by a standard electroporation procedure (17, 39), and then a hygromycin-resistant colony was selected. Complementation was confirmed by protein expression with Western blotting using anti-MDP1 MAb 3A (data not shown).

SEM analysis. Five-milliliter portions of culture aliquots were concentrated by centrifugation (3,000 × *g*) before suspension in fresh Middlebrook 7H9-ADC medium. The OD_{650} was adjusted to 0.1, and then the preparations were placed on poly-L-lysine-coated Thermanox coverslips in 24-well tissue culture plates. The bacteria were allowed to settle for 30 min before gentle decanting and addition of 1 ml of a solution containing 2% paraformaldehyde and 2.5% glutaraldehyde in 0.1 M sodium cacodylate buffer (pH 7.4) with 0.2 M sucrose. The samples were incubated at 4°C overnight before treatment with 2% OsO_4 in 0.1 M cacodylate buffer for 2 h at room temperature. A series of sequential ethanol dehydration steps were performed (50, 70, 95, and 100% ethanol, 10 min each) before samples were dried under CO_2 using a critical point drier (HCP-2; Hitachi). Samples were Pt-Pd sputter coated (E-1030; Hitachi) and imaged with an Hitachi S-4700 scanning electron microscope (SEM). The SEM analysis was performed in triplicate using three independently grown cultures.

Chase of glycolipid synthesis. *M. smegmatis* strains, including the wild type, the MDP1 KO mutant, and the complemented strain, were precultured at 37°C in LB broth (Sigma) containing 1-mm-diameter glass beads. First, bacterial clumps were disrupted with the beads by vortexing, and then the OD_{650} was adjusted to 0.1. Then 5 μl of each bacterial suspension was added to 5 ml of fresh medium containing glass beads. [1-^{14}C]acetic acid (sodium salt; 37 MBq/ml; PerkinElmer Life & Analytical Sciences, Massachusetts) was added at a final concentration of 1 μCi/ml on day 3 or 7. Each bacterial medium was incubated for 16 h and diluted to obtain 6.0×10^7 CFU/ml. Two milliliters of this bacterial suspension was collected by centrifugation and washed with pure water three times. After the supernatants were discarded, we added 1 ml of chloroform-methanol (3:1, vol/vol) and sonicated the preparation for 30 min. Thirty microliters of the chloroform layer was spotted on a TLC plate. The radioactivity of the separated spots was quantified by using the BAS system software as described above.

MALDI-TOF mass spectrometry analysis. A matrix-assisted laser desorption ionization–time of flight (MALDI-TOF) mass spectrometry analysis was carried out by using an Ultraflex mass spectrometer (Bruker Daltonics) in the reflectron mode. Samples were dissolved in chloroform-methanol (2: 1, vol/vol) at a concentration of 1 mg/ml and applied to the sample plate as droplets. 2,5-Dihydroxybenzoic acid was used as the matrix. The accelerating voltage was 20 kV.

Construction of BCG-Luc and assessment of its growth. Linker DNAs including the Shine-Dalgarno sequence (AGCTTAGTACTGGATCCGAGGACC TGCC and GATCGGCAGGTCCTCGGATCCAGTACTA) were synthesized by Sigma Genosys. pGEM-Luc (Promega) was digested with both BamHI and HindIII, and annealed linker DNA was inserted by ligation utilizing a ligation kit (version 1; Takara). The construct was then digested with HindIII and StuI, and the gene fragment containing the Shine-Dalgarno sequence and the luciferase gene was inserted into pSO246 (25), which had been digested with BamHI, blunt ended with T4 DNA polymerase, and digested with HindIII. The resulting plasmid was designated pSO-Luc. pMV261 (39) was digested with KpnI and HindIII, and the Hsp60 promoter region was inserted into the same site of pSO-Luc. The final construct was introduced into BCG by electroporation by the method described previously (25), and the kanamycin-resistant BCG-Luc strain was obtained. BCG-Luc was grown at 37°C in Middlebrook 7H9-ADC medium until mid-log phase and collected by centrifugation. Bacteria were suspended in RPMI 1640 (Sigma) containing 10% FBS with or without MDP1 or Ag85 complex proteins in a 96-well tissue culture plate (Becton Dickinson) and incubated at 37°C. Luciferase activity was determined at each time point as described previously (12).

Statistical analyses. Data were analyzed by using a Power Macintosh G5 and StatView 5.0 (SAS Institute Inc.) and were expressed as means ± standard deviations. Data that appeared to be statistically significantly different were compared by using an analysis of variance for comparing the means of multiple groups and were considered significantly different if the *P* value was less than 0.05.

RESULTS

MDP1 binds externally to the cell wall of BCG. MDP1 acts as an adhesin on the envelope through interaction with glycosaminoglycans on the host cell surface (1, 38). Because MDP1 is retained in the cell wall, we hypothesized that MDP1 is tightly bound to some unknown targets in the cell wall. In order to assess this possibility, first we examined the binding of MDP1 to the cell wall. We incubated FLUOS-labeled MDP1 with BCG and investigated the interaction by fluorescence microscopy. The results revealed that MDP1 (pI 12.4; molecular mass, 21 kDa) bound to the surface of BCG (Fig. 1A). In contrast, other FLUOS-labeled basic proteins, such as egg white lysozyme (pI 9.2; molecular mass, 16 kDa) (Fig. 1B) and bovine histone H1 (pI 11.5; molecular mass, 21 kDa) (Fig. 1C), did not interact with BCG. Bovine serum albumin (pI 5.4) did not interact either (data not shown). Thus, MDP1 can specifically bind externally to the cell wall.

MDP1 binds to TMM and TDM but not to free mycolic acids. Mycolic acids form an ordered structure in the envelope and are believed to be some of the outermost covalently linked elements (3, 20). *M. tuberculosis* produces three kinds of mycolic acids, the alpha-, methoxy-, and keto-mycolates. Three types of MAMEs (alpha-, methoxy-, and keto-mycolates), as well as TMM and TDM derived from *M. tuberculosis* strain Aoyama B, were immobilized on an ELISA plate and reacted with MDP1, and the interaction was detected with anti-MDP1 MAb 3A (subclass IgG1, light chain κ). The affinity of MAb 3A for MDP1 was 1.39 e^{-9} M as determined by surface plasmon resonance analysis with a Biacore biosensor (Biacore) (data not shown). This MAb binds to neither TMM nor TDM (data not shown). The results showed that MDP1 bound to TMM and TDM but not to any type of MAME (Fig. 1D). This indicates that MDP1 specifically recognizes the covalent linkage of mycolic acids to the 6-hydroxyl group of trehalose, because MDP1 does not bind to any mycolic acid (Fig. 1D) or free trehalose (1).

Physiological interaction between MDP1 and glycolipid in the mycobacterial cell wall. Next we examined whether MDP1 actually associated with TMM and TDM in the mycobacterial envelope by using an immunoprecipitation assay. A cell wall fraction derived from BCG by the method described previously (27) was incubated with MAb 3A or control mouse IgG. Then MDP1-bound glycolipids were precipitated with protein G-coupled beads, extracted with an organic solvent (chloroform-methanol, 3:1 [vol/vol]), and analyzed by TLC. Both TMM and TDM were precipitated by MAb 3A but not by control IgG (Fig. 1E), showing that MDP1 associated with TDM and TMM in the cell wall. The data also showed that MDP1 bound to other unknown lipids that migrated above TDM, as well as below TMM (Fig. 1E).